

Figure 2 Histopathology of systemic IgG4-related lymphadenopathy (interfollicular plasmacytosis type, atypical lymphoplasmacytic and immunoblastic proliferation-like feature, patient no. 6). (a) The lymph node showed atrophic germinal center with discrete mantle zone, and expansion of the interfollicular area. (b) High endothelial venules were prominent, and there was polymorphous cellular infiltration; plasma cells and immunoblasts were especially distinct (c) The interfollicular area showed heavy infiltration with mature plasma cells, plasmacytoid cells, small lymphocytes, and immunoblasts. (d) Eosinophil infiltration was recognized. Immunostaining of IgG4 (e) and IgG (f). The IgG4/IgG-positive cell ratio was 72.7%. (a–d) Hematoxylin and eosin staining; (a) 40, (b) 200, (c and d) 400, and (e and f) 100.

hypoalbuminemia, or hypocholesterolemia, and elevated interleukin-6 and C-reactive protein were the exceptions. These findings are quite different from those of multicentric Castleman's disease.<sup>15–18</sup>

Interleukin-6 is a multifunction cytokine that has various biological activities in target cells and regulates immune responses, acute phase reactions, hematopoiesis, and bone metabolism.<sup>25</sup> Dysregulated

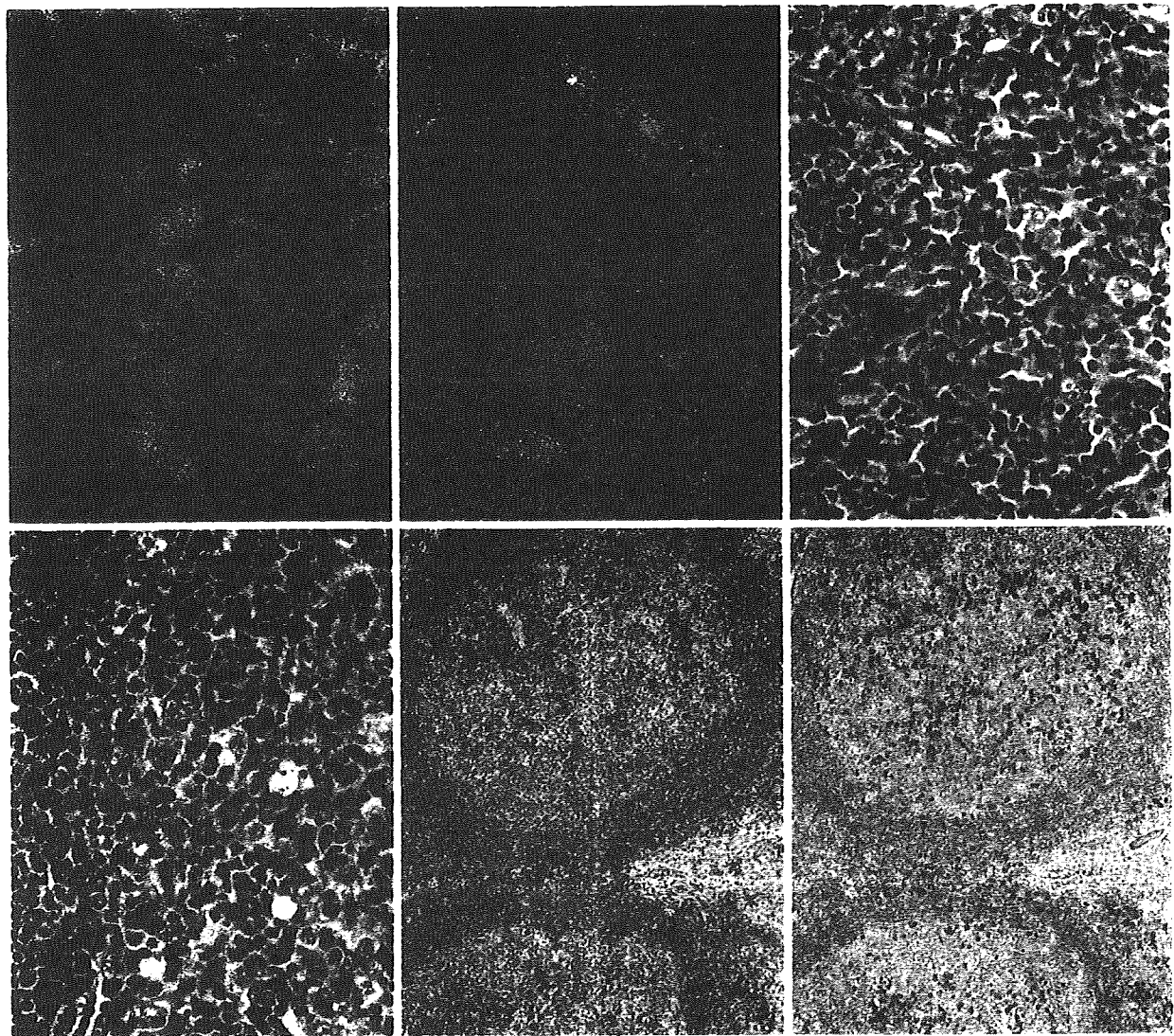


Figure 3 Histopathology of systemic IgG4-related lymphadenopathy (intra-germinal center plasmacytosis type, patient no. 9). (a and b) The lymph node showed numerous lymphoid follicles with hyperplastic germinal centers and a distinct mantle zone, with focal progressive transformation of germinal centers. (c) Eosinophils infiltrated the interfollicular area. (d) Plasma cells and plasmacytoid cells infiltrated the germinal center. Immunostaining of IgG4 (e) and IgG (f). IgG4-positive cells mainly infiltrated the germinal center, and the IgG4/IgG-positive cell ratio was 63.0%. (a–d) Hematoxylin and eosin staining; (a) 20, (b) 40, (c and d) 400, and (e and f) 100.

overproduction of interleukin-6 is found in autoimmune diseases, such as rheumatoid arthritis, multicentric Castleman's disease, and Crohn's disease.<sup>16–18,26,27</sup> C-reactive protein is a pentamer of 23-kd subunits that is synthesized and secreted by hepatocytes upon stimulation by a variety of inflammatory cytokines, including tumor necrosis factor- $\alpha$ , interleukin-1, and especially interleukin-6. Therefore, interleukin-6 is closely related to the production of C-reactive protein.<sup>25–29</sup> Accordingly, interleukin-6 and C-reactive protein may become considerably important as differential diagnostic markers between systemic IgG4-related lymphadenopathy and multicentric Castleman's disease. Masaki et al<sup>6</sup> have

reported that IgG4-related disease is not associated with an elevated serum interleukin-6 level, and cited measurement of serum interleukin-6 as an important tool of differential diagnosis. In our present series, two patients (nos. 2 and 4) showed slight, and one patient (no. 6) showed high elevation of serum interleukin-6, but their C-reactive protein levels were not as highly elevated as in multicentric Castleman's disease. Our patients using steroids showed a good response, and the histological findings of patient nos. 2 and 6 showed no similarities to those of Castleman's disease. The reference value of interleukin-6 is generically 0–4.0 pg/ml. However, Yokayama<sup>30</sup> has reported that the interleukin-6 value was over 25 pg/ml in 7% of the

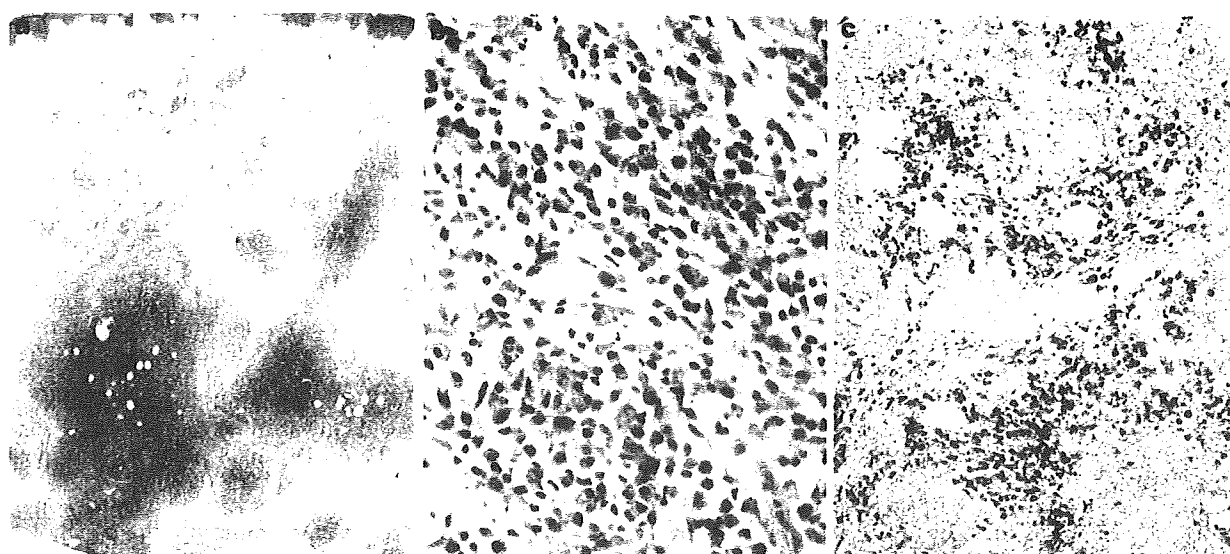


Figure 4 Histopathology of a skin lesion of a patient with systemic IgG4-related lymphadenopathy (patient no. 9). (a and b) Plasma cells, small lymphocytes and eosinophils showed a nodular-forming infiltration in the intermediate to deep dermis. (c) Immunostaining of IgG4; many plasma cells expressed IgG4. (a and b) Hematoxylin and eosin staining; (a) 20, (b) 400, and (c) 100.

healthy subjects. Therefore, interleukin-6 values might vary widely among individuals.

Our patients with systemic IgG4-related lymphadenopathy all showed hypergammaglobulinemia, but serum IgM and IgA was normal in almost all patients. In contrast, multicentric Castleman's disease is characterized by increased serum IgG, IgM, and IgA levels,<sup>16</sup> which are caused by the increase in serum interleukin-6.<sup>5</sup> In this series, most patients showed cervical, hilar, mediastinal, and para-aortic lymph node swelling, and the lymph nodes were generally not very large (up to 2 cm). These findings were consistent with previous reports of IgG4-related lymphadenopathy.<sup>3,4,11</sup>

Histologically, we could classify the cases into two types based on the infiltration pattern of IgG4-positive cells: interfollicular plasmacytosis type and intra-germinal center plasmacytosis type. Morphologically, the interfollicular plasmacytosis type was characterized by expansion of the interfollicular area, moderate to marked increase in vascularity, and infiltration of IgG4-positive cells mainly in the interfollicular area. Five out of six cases showed eosinophil infiltration in the interfollicular area. These cases demonstrated Castleman disease-like features (patient nos. 1, 3, and 4) or atypical lymphoplasmacytic and immunoblastic proliferation-like features (patient nos. 2, 5, and 6). Koo et al<sup>23</sup> reported that atypical lymphoplasmacytic and immunoblastic proliferation is unusual in cases of lymph node lesion associated with various autoimmune diseases, including rheumatoid arthritis. Histopathologically, the lesion is characterized by prominent lymphoplasmacytic infiltration with various number of immunoblasts.<sup>23,24</sup> In this series,

three patients showed this pattern, but there was no evidence of rheumatoid arthritis. In addition, there was abundant IgG4-positive cells infiltration in the lesion and the serum IgG4 value was elevated. These findings are consistent with IgG4-related disease. These results suggested that some IgG4-related lymphadenopathy might be confused with multicentric Castleman's disease or atypical lymphoplasmacytic and immunoblastic proliferation. In the case of systemic IgG4-related lymphadenopathy of atypical lymphoplasmacytic and immunoblastic proliferation type, the histology can be confused with that of malignant lymphoma, especially angioimmunoblastic T-cell lymphoma. However, the former has no clear cells, no CD10-positive T-cells, no extrafollicular follicular dendritic cell proliferation, and no T-cell receptor gamma gene rearrangement.

By contrast, the intra-germinal center plasmacytosis type shows marked follicular hyperplasia, a mild increase in vascularity, and IgG4-positive cells mainly infiltrating the germinal centers. In our study, the two patients with this type showed progressively transformed germinal center. The germinal centers are known to be a major site for B-cell selection. In the germinal centers, B cells perform numerous somatic hypermutations and heavy-chain class-switches and only a portion of them are selected through the cooperation of T cells and follicular dendritic cells. The selected B cells exit the germinal centers and become plasma cells.<sup>31</sup> Therefore, the fact that many IgG4-producing plasma cells were found selectively in the germinal centers of our patients was a unique feature. The mechanisms involved in this feature are not clear.

Zen et al<sup>10</sup> have reported that the expressions of T helper (Th) 2 cytokines (interleukin-4, interleukin-5, and interleukin-13) and regulatory cytokines (interleukin-10 and transforming growth factor- $\beta$ ) were upregulated in the affected tissues of patients with IgG4-related sclerosing pancreatitis and cholangitis. They have suggested that the prominent Th2 and regulatory immune reactions in this disease might indicate that its pathogenesis involves an allergic mechanism. In addition, they described that interleukin-10 has a major role in directing B-cells to produce IgG4.<sup>10</sup> Therefore, interleukin-10 might induce differentiation of B cells into IgG4-positive plasma cells in the germinal centers. At any rate, this unique histological feature could be a special finding for IgG4-related lymphadenopathy.

Interestingly, eight of our nine cases (89%) of systemic IgG4-related lymphadenopathy showed eosinophil infiltration. Zen et al<sup>10</sup> reported that eosinophils infiltrated in the affected tissues in their patients with IgG4-related sclerosing pancreatitis and cholangitis. As previously mentioned, Th2 cytokines (interleukin-4, interleukin-5, and interleukin-13) were upregulated in the affected tissues of patients with IgG4-related disease. Interleukin-5 and interleukin-13 were activated by eosinophil infiltration and IgE production. Masaki et al<sup>6</sup> have reported that serum IgE level is elevated in IgG4-related diseases. In our series, the serum IgE value was significantly elevated in the examined patients. So, the findings of eosinophilic infiltration and serum IgE value elevation might be a specific finding of IgG4-related disease.

Little is known about the lymphomagenesis of IgG4-related disease. We recently reported the first case of marginal zone B-cell lymphoma arising from ocular adnexal IgG4-related disease<sup>7</sup> and IgG4-producing marginal zone B-cell lymphoma.<sup>32</sup> However, the present series showed no immunoglobulin light-chain restriction and no immunoglobulin heavy chain gene rearrangement.

In conclusion, in systemic IgG4-related disease, C-reactive protein and interleukin-6 are usually not elevated. Systemic IgG4-related disease and multicentric Castleman's disease showed overlapping but somewhat distinct pathologic findings, and serum data (especially C-reactive protein and interleukin-6) are useful to differentiate between them. Eosinophilic infiltration and serum IgE value elevation might be a specific feature of IgG4-related lymphadenopathy.

### Disclosure/conflict of interest

The authors have no potential conflicts of interest.

### References

- 1 Hamano H, Kawa S, Horiuchi A, et al. High serum IgG4 concentrations in patients with sclerosing pancreatitis. *N Engl J Med* 2001;344:732–738.

- 2 Hamano H, Kawa S, Ochi Y, et al. Hydronephrosis associated with retroperitoneal fibrosis and sclerosing pancreatitis. *Lancet* 2002;359:1403–1404.
- 3 Kamisawa T, Okamoto A. IgG4-related sclerosing disease. *World J Gastroenterol* 2008;14:3948–3955.
- 4 Kamisawa T, Nakajima H, Egawa N, et al. IgG4-related sclerosing disease incorporating sclerosing pancreatitis, cholangitis, sialadenitis and retroperitoneal fibrosis with lymphadenopathy. *Pancreatol* 2006;6:132–137.
- 5 Kojima M, Miyawaki S, Takada S, et al. Lymphoplasmacytic infiltrate of regional lymph nodes in Küttner's tumor (chronic sclerosing sialadenitis): a report of 3 cases. *Int J Surg Pathol* 2008;16:263–268.
- 6 Masaki Y, Dong L, Kurose N, et al. Proposal for a new clinical entity, IgG4-positive multi-organ lymphoproliferative syndrome: analysis of 64 cases of IgG4-related disorders. *Ann Rheum Dis* 2008 published online 13 Aug 2008; doi: 10.1136/ard.2008.089169.
- 7 Sato Y, Ohshima K, Ichimura K, et al. Ocular adnexal IgG4-related disease has uniform clinicopathology. *Pathol Int* 2008;58:465–470.
- 8 Zhang L, Notohara K, Levy MJ, et al. IgG4-positive plasma cell infiltration in the diagnosis of autoimmune pancreatitis. *Mod Pathol* 2007;20:23–28.
- 9 Zen Y, Fujii T, Sato Y, et al. Pathological classification of hepatic inflammatory pseudotumor with respect to IgG4-related disease. *Mod Pathol* 2007;20:884–894.
- 10 Zen Y, Fujii T, Harada K, et al. Th2 and regulatory immune reactions are increased in immunoglobulin G4-related sclerosing pancreatitis and cholangitis. *Hepatology* 2007;45:1538–1546.
- 11 Cheuk W, Yuen HKL, Chu SYY, et al. Lymphadenopathy of IgG4-related sclerosing disease. *Am J Surg Pathol* 2008;32:671–681.
- 12 Castleman B, Iverson L, Menendez VP. Localized mediastinal lymph-node hyperplasia resembling thymoma. *Cancer* 1956;9:822–830.
- 13 Flendrig JA, Schillings PHM. Benign giant lymphoma: the clinical signs and symptoms. *Folia Med Neerl* 1969;12:119–120.
- 14 Keller AR, Hochholzer L, Castleman B. Hyaline-vascular and plasma-cell types of giant lymph node hyperplasia of the mediastinum and other locations. *Cancer* 1972;29:670–683.
- 15 Frizzera G, Peterson BA, Bayrd ED, et al. A systemic lymphoproliferative disorder with morphologic features of Castleman's disease: clinical findings and clinicopathologic correlations in 15 patients. *J Clin Oncol* 1985;3:1202–1216.
- 16 Nishimoto N, Kanakura Y, Aozasa K, et al. Humanized anti-interleukin-6 receptor antibody treatment of multicentric Castleman's disease. *Blood* 2005;106:2627–2632.
- 17 Kojima M, Nakamura S, Shimizu K, et al. Clinical implication of idiopathic plasmacytic lymphadenopathy with polyclonal hypergammaglobulinemia: a report of 16 cases. *Int J Surg Pathol* 2004;12:25–30.
- 18 Kojima M, Nakamura N, Tsukamoto N, et al. Clinical implication of multicentric Castleman's disease among Japanese: a report of 28 cases. *Int J Surg Pathol* 2008;16:391–398.
- 19 Mannami T, Yoshino T, Oshima K, et al. Clinical, histopathological, and immunogenetic analysis of ocular adnexal lymphoproliferative disorders: characterization of malt lymphoma and reactive lymphoid hyperplasia. *Mod Pathol* 2001;14:641–649.

- 20 Sato Y, Nakamura N, Nakamura S, et al. Deviated VH4 immunoglobulin gene usage is found among thyroid mucosa-associated lymphoid tissue lymphomas, similar to the usage at other sites, but is not found in thyroid diffuse large B-cell lymphomas. *Mod Pathol* 2006;19:1578–1584.
- 21 Sato Y, Ichimura K, Tanaka T, et al. Duodenal follicular lymphomas share common characteristics with mucosa-associated lymphoid tissue lymphomas. *J Clin Pathol* 2008;61:377–381.
- 22 Dongen JV, Langerak AW, Brüggemann M, et al. Design and standardization of PCR primers and protocols for detection of clonal immunoglobulin and T-cell receptor gene recombinations in suspect lymphoproliferations: report of the BIOMED-2 action BMH4-CT98-3936. *Leukemia* 2003;17:2257–2317.
- 23 Koo CH, Nathwani BN, Winberg CD, et al. Atypical lymphoplasmacytic and immunoblastic proliferation in lymph nodes of patients with autoimmune disease (autoimmune-disease-associated lymphadenopathy). *Medicine (Baltimore)* 1984;64:274–290.
- 24 Kojima M, Motoori T, Hosomura Y, et al. Atypical lymphoplasmacytic and immunoblastic proliferation from rheumatoid arthritis: a case report. *Pathol Res Pract* 2006;202:51–54.
- 25 Usón J, Balsa A, Pascual-Salcedo D. Soluble interleukin 6 (IL-6) receptor and IL-6 levels in serum and synovial fluid of patients with different arthropathies. *J Rheumatol* 1997;24:2069–2075.
- 26 Nishimoto N, Terao K, Mima T, et al. Mechanisms and pathological significances in increase in serum interleukin-6 (IL-6) and soluble IL-6 receptor after administration of anti-IL-6 receptor antibody, tocilizumab, in patients with rheumatoid arthritis and Castleman's disease. *Blood* 2008;112:3959–3964.
- 27 Castell JV, Gómez-Lechón MJ, David M, et al. Recombinant human interleukin-6 (IL-6/BSF-2/HSF) regulates the synthesis of acute phase proteins in human hepatocytes. *FEBS Lett* 1988;232:347–350.
- 28 Castell JV, Gómez-Lechón MJ, David M, et al. Acute-phase response of human hepatocytes: regulation of acute-phase protein synthesis by interleukin-6. *Hepatology* 1990;12:1179–1186.
- 29 Gabay C, Kushner I. Acute-phase proteins and other systemic responses to inflammation. *N Eng J Med* 1999;340:448–454.
- 30 Yokoyama A. Interleukin-6 (IL-6) / soluble IL-6 receptor. *Nippon Rinsho* 2005;63:72–74.
- 31 Kondo E, Nakamura S, Onoue H, et al. Detection of bcl-2 protein and bcl-2 messenger RNA in normal and neoplastic lymphoid tissues by immunohistochemistry and in situ hybridization. *Blood* 1992;80:2044–2051.
- 32 Sato Y, Takata K, Ichimura K, et al. IgG4-producing marginal zone B-cell lymphoma. *Int J Hematol* 2008;88:428–433.



# Duodenal and nodal follicular lymphomas are distinct: the former lacks activation-induced cytidine deaminase and follicular dendritic cells despite ongoing somatic hypermutations

Katsuyoshi Takata<sup>1</sup>, Yasuharu Sato<sup>1</sup>, Naoya Nakamura<sup>2</sup>, Yara Yukie Kikuti<sup>2</sup>, Koichi Ichimura<sup>1</sup>, Takehiro Tanaka<sup>1</sup>, Toshiaki Morito<sup>1</sup>, Maiko Tamura<sup>1</sup>, Takashi Oka<sup>1</sup>, Eisaku Kondo<sup>1</sup>, Hiroyuki Okada<sup>3</sup>, Akira Tari<sup>4</sup> and Tadashi Yoshino<sup>1</sup>

<sup>1</sup>Department of Pathology, Okayama University Graduate School of Medicine Dentistry and Pharmaceutical Sciences, Okayama, Japan; <sup>2</sup>Department of Pathology, Tokai University School of Medicine, Isehara, Kanagawa, Japan; <sup>3</sup>Department of Gastroenterology and Hepatology, Okayama University Graduate School of Medicine Dentistry and Pharmaceutical Sciences, Okayama, Japan and <sup>4</sup>Department of Internal Medicine, Hiroshima Red Cross Hospital and Atomic-Bomb Survivors Hospital, Hiroshima, Japan

Although most follicular lymphomas are believed to be of nodal origin, they sometimes originate from the duodenum. We have reported that the latter differ from nodal follicular lymphomas in having lower clinical stages and uniformly low histological grades, along with variable region of immunoglobulin heavy chain gene (VH) usage that is more similar to mucosa-associated lymphoid tissue (MALT) lymphomas. Little is known, however, about whether they possess other characteristics of nodal follicular lymphomas, particularly ongoing mutations with follicular dendritic cells. We examined 17 cases for which PCR identified the monoclonal bands of the immunoglobulin gene. The duodenal cases showed ongoing mutations, but they lacked activation-induced cytidine deaminase (AID) expression, a statistically significant difference from the nodal cases ( $P < 0.001$ ), and their follicular dendritic cell networks were disrupted. Moreover, not only were VH deviations observed but also they used very restricted VH genes. Although the mechanisms of ongoing mutation without AID and follicular dendritic cell were not clarified, restricted VH usage strongly suggested that antigen stimulation was involved, and that was similar to MALT lymphomas. In conclusion, duodenal follicular lymphomas were shown to be unique, in that they had ongoing hypermutations such as nodal cases, but the mechanisms involved in the hypermutation were quite different; furthermore, restricted VH usage suggested a strong similarity to the antigen-dependent origin of MALT lymphomas.

Modern Pathology (2009) 22, 940–949; doi:10.1038/modpathol.2009.51; published online 24 April 2009

Keywords: duodenal follicular lymphoma; AID; follicular dendritic cell

We have reported that duodenal follicular lymphomas are frequently found in the second portion of the duodenum.<sup>1</sup> Although they express CD10 and bcl-2 and harbor t(14;18) translocation similar to nodal follicular lymphomas,<sup>2</sup> most of them are obviously at lower clinical stages than the nodal cases (most are stage I–II) and have lower histolo-

gical grading with rather dominantly uniform intermediate small cleaved cells.

The vast majority of follicular lymphomas originate from lymph nodes, and earlier reports have clearly indicated that these follicular lymphoma cells derive from germinal-center B cells: both cells share characteristics such as accumulation of somatic hypermutation and ongoing mutations.<sup>3</sup> Furthermore, they interact with follicular dendritic cells. In an earlier report, we also described that duodenal follicular lymphomas have a high frequency of IgVH4 gene usage as in mucosa-associated lymphoid tissue (MALT) lymphomas, with which they share other characteristics.<sup>4–6</sup> Localized disease is one of main characteristics of MALT lymphomas.

Correspondence: Professor T Yoshino, MD, PhD, Department of Pathology, Okayama University Graduate School of Medicine, Dentistry and Pharmaceutical Sciences, 2-5-1 Shikata-cho, Okayama city, Okayama, 700-8558, Japan.  
E-mail: yoshino@md.okayama-u.ac.jp  
Received 25 January 2009; revised 24 February 2009; accepted 25 February 2009; published online 24 April 2009

From these findings, we considered whether duodenal follicular lymphomas have other differences from nodal follicular lymphomas, and decided to examine their expression of activation-induced cytidine deaminase (AID), which plays the important roles of class-switch recombination and somatic hypermutation,<sup>7</sup> and the patterning of their follicular dendritic cell networks. It is reported that AID expression is associated with ongoing mutation in nodal follicular lymphoma,<sup>8</sup> but is not correlated with diffuse large B-cell lymphomas.<sup>9</sup> Although other characteristics of duodenal follicular lymphomas have been described, to the best of our knowledge no report has focused on their somatic and ongoing mutations, which are the most important similarity to germinal-center B-cell lymphomas.

In this report, we discovered that duodenal follicular lymphomas showed ongoing somatic hypermutations similar to nodal cases; unlike the latter, however, they lack AID and have disrupted follicular dendritic cell networks.

## Materials and methods

### Patient Selection

Buffered formalin-fixed and paraffin-embedded tissues (10%) were used for histological, immunohistochemical and immunogenotypical studies. We chose 30 consecutive patients of duodenal follicular lymphoma, successfully amplified the monoclonal rearranged band of the VH gene in 17 of these patient samples, and focused on these samples for further analyses. Informed consent for examination was obtained for the use of all samples.

### Immunohistochemistry

Formalin-fixed, paraffin-embedded tissue sections were subjected to immunohistochemical staining. Staining was carried out using heat-induced epitope retrieval or trypsin-induced retrieval, an avidin-biotin complex method, and an automated immunostainer (Ventana Medical System, Tuscon, AZ, USA), as described earlier.<sup>10</sup> The antibody panel used to assess these cases was as follows (clone, dilutions): CD20 (L26, 1:200), CD3 (PS-1, 1:50), CD10 (56C6, 1:50), CD5(4C7, 1:100), bcl-2 (3.1, 1:200), CD23 (1B12, 1:100) and Ki-67 (MIB-1, 1:5000) (Novocastra, Newcastle-upon-Tyne, UK); CD21 (1F8, 1:20), MUM1 (MUM1p, 1:50) (DAKO Cytomation, Glostrup, Denmark A/S); bcl-6 (D-8, 1:100) (Santa Cruz, CA, USA); and cyclin D1 (SP4, ready to use) (Nichirei, Tokyo, Japan); AID (ZA001, 1:100) (ZYMED, South San Francisco, CA, USA). As for CD20, CD3, CD10, CD5, cyclin D1, bcl-2, bcl-6 and MUM-1 antigens, positivity was determined when 30% or more lymphoma cells were positive for their antibodies. For AID expression in tumor

follicles, samples with 20% or more expressing cells were evaluated as positive. Ki-67-positive cells were counted in tumor follicles.

### DNA Extraction and PCR

DNA was extracted from paraffin-embedded tissue using the QIAamp DNA Micro Kit- (Qiagen Inc., Valencia, CA, USA). The variable region (CDR2 and FW3) and VDJ region (CDR3) of the immunoglobulin heavy-chain gene were amplified by semi-nested PCR, using the primers of FR2, LJH and VLJH as described earlier.<sup>11,12</sup> Primers were as follows: 5<sup>′</sup>-CCGGRAARRGTCTGGAGTGG-3<sup>′</sup>, as upstream consensus V region primer (FR2); 5<sup>′</sup>-CTTACCTGAGGAGACGGTGACC-3<sup>′</sup>, as a consensus J region primer (LJH); 5<sup>′</sup>-GTGACCAGGGTNCCTTGGCCCC-3<sup>′</sup>, as a consensus J region primer (VLJH). PCR products were purified using the QIAquick PCR purification kit (Qiagen). Then 1 ml of the PCR product was applied for direct sequencing (ABI PRISM Model 3100, version 3.7, Applied Biosystems).

### Ongoing Mutation Study and Analysis

PCR products were ligated into the pDrive cloning vector and transformed into DH5alpha cells (TaKaRa Bio. Inc., Tokyo, Japan) according to the instruction manual (PCR cloning kit, Qiagen). After an overnight culture, 10 and more white colonies were picked from a Luria-Bertani (LB) agar plate based on the X-Gal screening, then placed into 25 ml of the Insert Check ready kit solution (TOYOBO, Osaka, Japan). PCR conditions consisted of 30 cycles of 94°C for 30 s, 60°C for 5 s and 72°C for 30 s. Ten samples including correct PCR products confirmed by checking 2% gel electrophoresis for each case were sequenced by the same method as described above. Then, the closest germline was searched for by BLAST using the immunoglobulin sequence (NCBI). Ongoing mutation was determined by dividing the cumulative number of partially shared mutations (mutations shared by some clones but not by all the VH gene clones) and unique mutations (mutations unique to a distinct VH gene clone) with the expected number of mutations calculated based on the PCR error rate ( $4.5 \times 10^{-4}$  change per base per PCR cycle) by the method described above.<sup>7</sup> The  $w^2$  test with Yates' correction when appropriate was used to evaluate the association of qualitative variables in the different groups. Statistical analysis was carried out using Statcel2 for Windows. Values of  $P < 0.05$  were considered statistically significant.

### Fluorescence In Situ Hybridization

Fluorescence in situ hybridization (FISH) for t(14;18)(q32;q21)/IGH-BCL2 translocations were

carried out using the BCL2 FISH DNA split signal probe (DAKO Cytomation, Glostrup, Denmark A/S) according to the manufacturer's instructions. We

examined FISH directly on paraffin-embedded tissue sections and detected split signal of BCL2 gene as described earlier.<sup>13</sup>

Table 1 Clinicopathologic features of duodenal follicular lymphoma

Patient no.	Age/sex	Stage	Grade	CD5	CyclinD1	CD10	bcl-2	bcl-6	MUM-1	t(14;18)	CD21 pattern
1	75/M	I	1			+	+	+		Not tested	Duodenal
2	57/M	I	1			+	+	+		Not tested	Duodenal
3	58/M	IV	1			+	+	+		+	Duodenal
4	75/M	II2	1			+	+	+			Duodenal
5	71/F	I	1			+	+	+		+	Duodenal
6	66/F	I	1			+	+	+			Nodal
7	51/M	I	1			+	+	+		+	Duodenal
8	49/M	II2	1			+	+	+		+	Duodenal
9	62/F	II2	1			+	+	+		+	Duodenal
10	54/M	I	1			+	+	+		+	Duodenal
11	61/F	IV	1			+	+	+		+	Duodenal
12	53/F	II2	1			+	+	+		+	Duodenal
13	57/F	I	2			+	+	+		+	Duodenal
14	56/M	II2	1			+	+	+		+	Duodenal
15	66/F	II2	1			+	+	+		+	Duodenal
16	55/F	II2	1			+	+	+		+	Nodal
17	63/F	II2	1			+	+	+		+	Duodenal

F, female; M, male.

Immunophenotypic data were analyzed using immunohistochemistry.

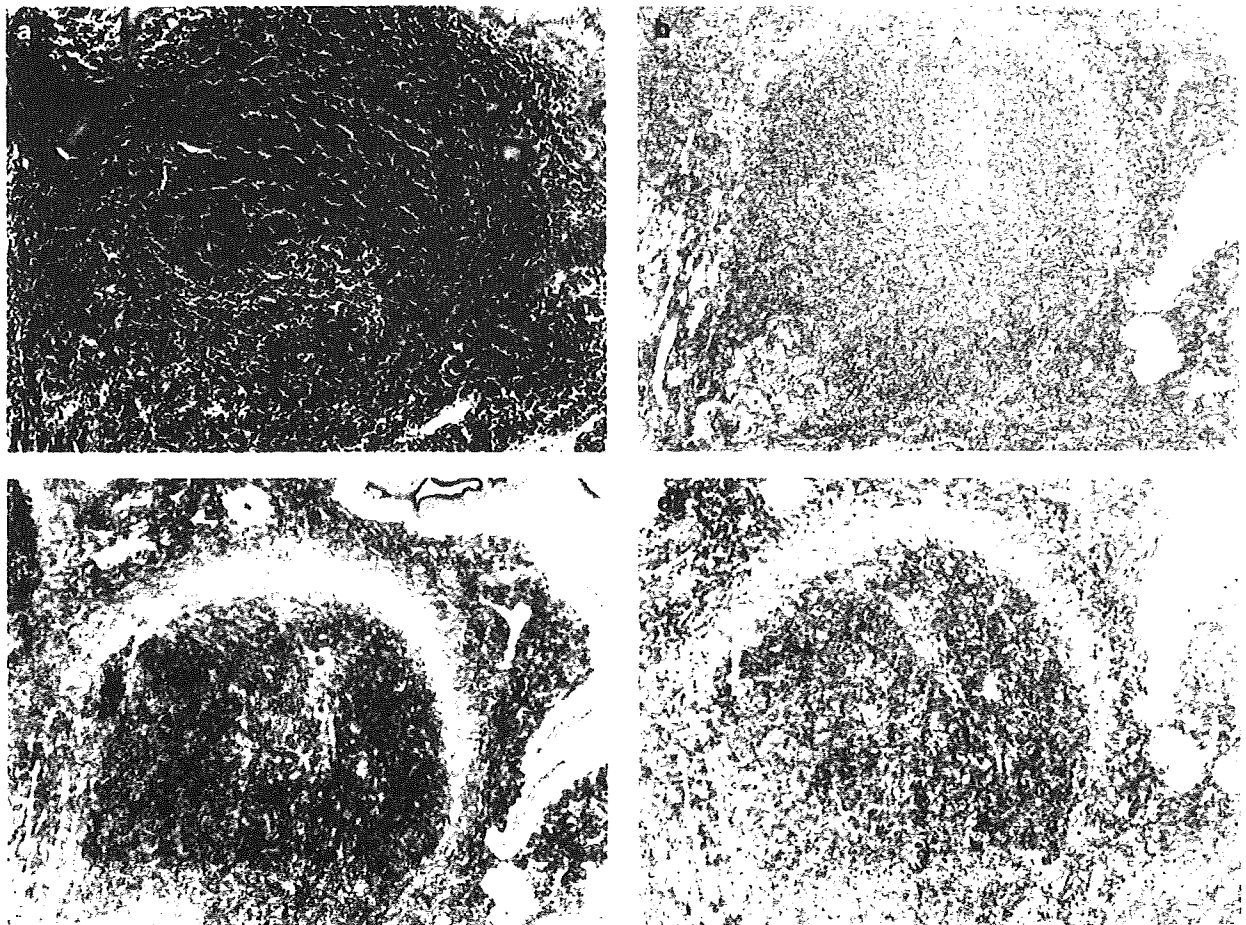


Figure 1 Duodenal follicular lymphoma and immunohistochemical stain (patient no.17). (a) H&E: A neoplastic follicle is composed of uniform intermediate small-cleaved cells. (b) Tumor cells are positive for CD20 in all cases (c) and for CD10 (d) and bcl-2.



## Results

### Patient Summary and CD21 Expression

Clinical features (age, gender, clinical stage) and the results of immunohistochemical study are shown in Table 1. The 17 patients (8 males and 9 females) ranged in age from 49 to 75 years with a median age of 61 years. According to the International Workshop (Lugano) Classification, seven cases were clinical stage I, eight cases were stage II and two cases were stage IV.<sup>14</sup> Histological grade were 1–2 of all cases. All patient samples expressed CD20, CD10, bcl-2 and bcl-6, and were negative for CD5, MUM1 and cyclin D1 by immunohistochemical study (Figure 1). In all cases, the Ki-67 labeling index was 0–10%. The presence of a t(14;18)(q32;q21)/IGH-BCL2 was sought by FISH depending on the material available. The translocation of 18q21 was detected in 13 of 15 (86.7%) cases (Figure 2 shows the split signal of patient no. 7 sample). We could not detect translocations at two patients' materials.

A typical pattern of follicular dendritic cells expressing CD21 and CD23 in nodal follicular lymphoma is shown in Figure 3 and clearly indicates neoplastic follicles. Nodal follicular lymphoma interacts with follicular dendritic cells, which sometimes provides a diagnostic clue.<sup>15</sup> On the contrary, out of 17 samples of duodenal follicular lymphomas, 15 showed a very similar pattern of follicular dendritic cells: they were rather densely arranged at the periphery of the neoplastic follicle area but few follicular dendritic cells were detected at the center of the neoplastic follicle area.

In most nodal follicular lymphomas, follicular dendritic cell networks occupied more than two-thirds of the neoplastic follicle areas. On the contrary, follicular dendritic cell networks occupied 0–10% of the neoplastic follicle areas in duodenal follicular lymphomas, and were distributed in the periphery of the neoplastic follicles. Accordingly, the nodal pattern was identified as neoplastic follicles coextensive with large follicular dendritic cell networks, whereas the duodenal pattern was

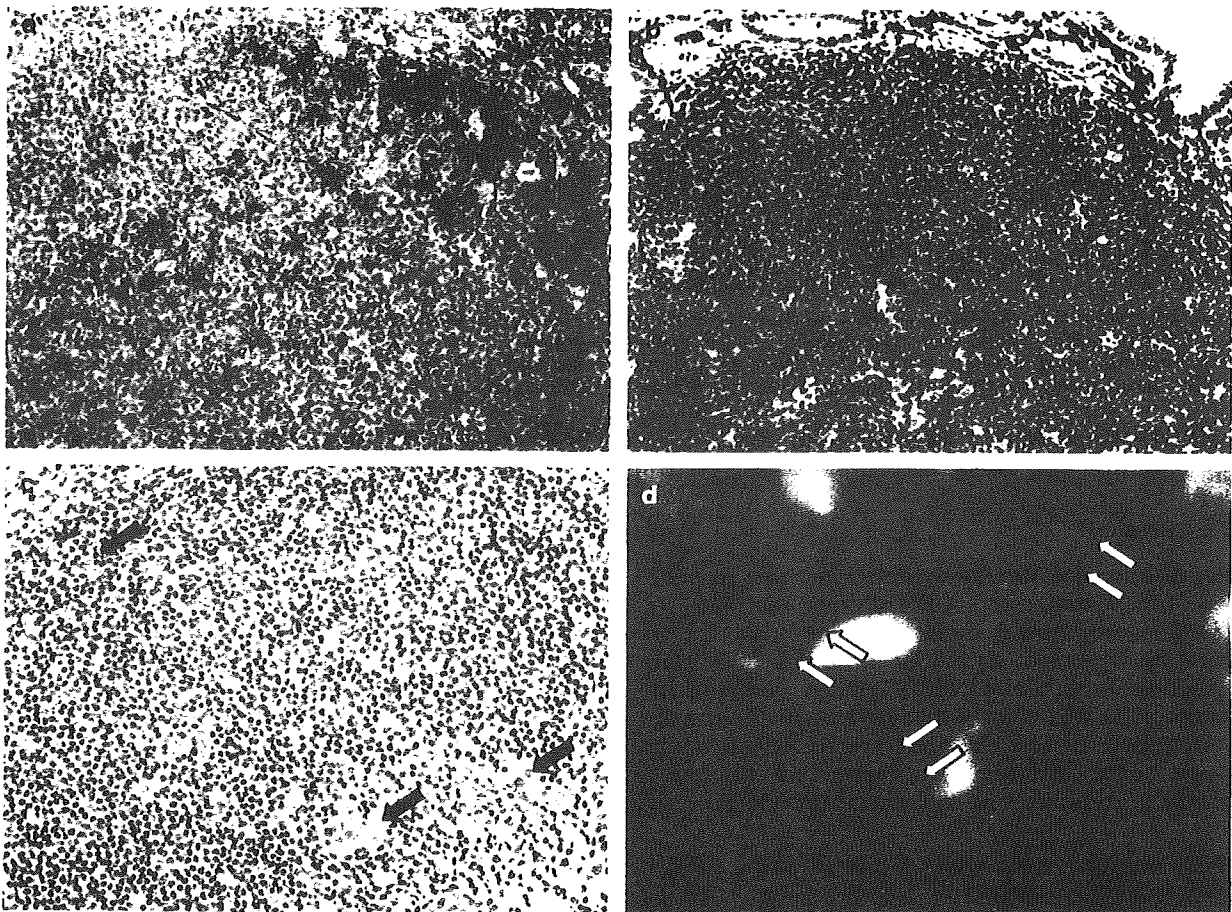


Figure 2 Expression of AID and FISH. (a) AID expression in nodal follicular lymphoma, grade 1. More than 20% of neoplastic cells are positive. (b) AID expression in duodenal follicular lymphoma (patient no. 8). Almost all neoplastic cells are negative. (c) AID expression in patient no. 2. Some positive cells are shown (arrows). (d) BCL2 split signal of patient no. 7 (arrows: The FISH DNA probes are a mixture of a Texas Red-labeled DNA probe (bcl-2-upstream) and a fluorescein-labeled DNA probe (bcl-2-downstream). Split signals of red- and green-labeled probe are seen in the lymphoma cells, indicating breaking apart of the bcl-2 gene.

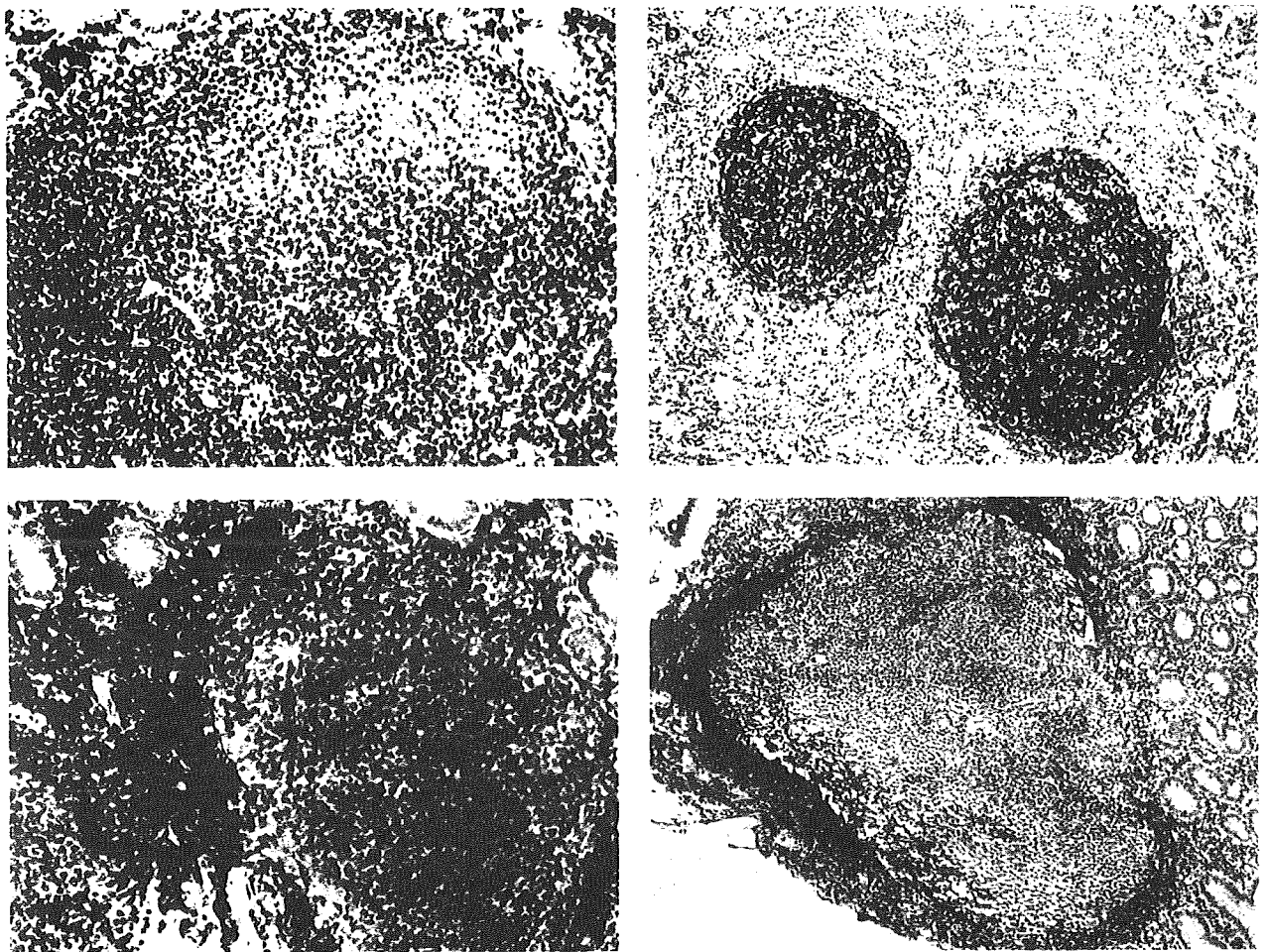


Figure 3 Expression of bcl-6, CD21 and CD23. (a) Tumor cells are positive for bcl-6 in all cases (shows patient no. 8). (b) CD21 expression in nodal follicular lymphoma, grade 1. Follicular dendritic cells are densely found in neoplastic follicles. (c) CD23 expression in duodenal follicular lymphoma (patient no. 17). Follicular dendritic cells are arranged at the periphery of the neoplastic follicle. (d) CD21 expression in other case of duodenal follicular lymphoma. Similar to CD23 expression.

identified as neoplastic follicles with disrupted, peripheral follicular dendritic cell networks.

**AID Expression**

In the duodenal follicular lymphomas, one patient sample (no. 9) expressed AID but other samples (16 samples) were almost completely negative for it (Figure 2). By contrast, out of 19 nodal follicular lymphomas, which histological grades were 1–2 in all cases, AID was clearly detected in 16 (Figure 2, data not shown). The difference in AID expression between nodal follicular lymphoma and duodenal follicular lymphoma was significant ( $P = 0.001$ ).

**Relationship among Follicular Dendritic Cells, AID, VH and Ongoing Mutation**

The VH gene usage and analysis of somatic hypermutation are shown in Table 2. We sequenced 17 cases of duodenal follicular lymphoma. The VH gene usage included 9 (53%) samples of VH3, 5

(29%) samples of VH4 and 3 (18%) samples of VH5. The distribution of mutations in CDR2 and FR3 are also shown in Table 2. Regardless of AID expression, all samples displayed somatic hypermutation; the mutation frequency was 0.7–15.6%, with an average of 9.1%. In VH5 usage cases, there tended to be a low mutation frequency (0.7–8.8%, average 3.8%).

In Table 3, most samples showed ongoing mutations, yielding an average of 19.6-fold more mutations than the expected number of additional mutations because of PCR error. Two AID-negative samples (no. 8 and no. 12) did not have any partially shared or unique mutations. Table 4 shows the nucleotide sequence of the VH gene of patient nos. 12 and 7. In no. 7, there were four partially shared mutation and five unique mutations.

**Discussion**

Follicular lymphoma is one of the most frequent indolent lymphomas, and most of them are of nodal

Table 2 AID expression and immunoglobulin gene analysis

Patient no.	AID expression <sup>a</sup>	VH usage	Number of bases analyzed	CDR2		FR3		Total		Mutation rate (%) <sup>b</sup>
				R	S	R	S	R	S	
1		VH3-73	153	6	1	7	2	15	3	11.8
2		VH3-48	147	3	1	1	3	4	4	5.4
3		VH3-72	153	7	0	5	4	12	4	10.5
4		VH4-34	140	5	0	7	2	12	2	10
5		VH5-a	147	0	0	1	0	1	0	0.7
6		VH3-73	141 <sup>c</sup>	6	0	6	1	12	1	9.3
7		VH4-b	144	7	0	7	2	14	2	11.1
8		VH4-39	144	4	0	6	4	10	4	9.7
9	+	VH3-15	153	8	0	2	6	10	6	10.5
10		VH5-51	147	2	0	1	0	3	0	2
11		VH5-51	147	3	2	5	3	8	5	8.8
12		VH4-61	144	2	1	2	1	4	2	4.2
13		VH4-39	144	6	1	3	3	9	4	9
14		VH3-73	153	7	2	3	3	10	5	9.8
15		VH3-23	147	12	0	8	3	20	3	15.6
16		VH3-23	147	6	3	5	3	11	6	11.6
17		VH3-23	147	9	2	8	2	17	4	14.3

CDR, complementary determining region; FR, framework region; R, replacement mutation; S, silent mutation.

<sup>a</sup>Immunohistochemically positive 4/20% in tumor follicles.

<sup>b</sup>Dividing the total number of R and S mutations in CDR2 and FR3 by the number of bases analyzed.

<sup>c</sup>In patient no. 6, deletion of nine nucleotides were found.

Table 3 AID expression and ongoing mutation in duodenal follicular lymphoma

Patient no.	AID expression	Number of clones analyzed	Number of bases sequenced	Point mutations				Number of mutations expected by PCR error	Ongoing mutation
				Total	Shared	Partially shared	Unique		
1		10	153	23	16	1	6	0.31	22.6
2		10	147	10	7	1	2	0.135	22.2
3		9	153	18	15	2	1	0.24	12.5
4		10	140	18	14	0	4	0.22	18.2
5		10	147	6	1	0	5	0.081	61.7
6		10	141	21	14	4	3	0.28	25
7		8	144	21	12	4	5	0.28	32.1
8		10	144	15	15	0	0	0.2	0
9	+	10	153	18	17	0	1	0.24	4.2
10		8	147	6	3	0	3	0.081	37
11		7	147	14	13	0	1	0.19	5.3
12		9	144	6	6	0	0	0.081	0
13		9	144	19	14	0	5	0.26	19.2
14		10	153	19	15	0	4	0.26	15.4
15		10	147	31	23	8	8	0.42	38.1
16		10	147	22	19	0	3	0.3	10
17		10	147	24	21	1	2	0.32	9.4

origin. But recently, intestinal (especially duodenal) follicular lymphomas have appeared with more frequency, and these are considered variants of follicular lymphoma in the fourth WHO classification.<sup>16</sup> Interestingly, from our surgical files, only 5.8% (17/290 cases) of follicular lymphomas were extranodal up to 2001, whereas 30.8% (153/497 cases) were extranodal in 2002–2007. This frequency needs to be investigated hereafter, but consultation from other institution to our

department has not changed in the past 10 years, hence this frequency indicates that intestinal follicular lymphomas have become popular and the incidence of finding them is increasing. The similarity of duodenal follicular lymphomas to MALT lymphomas has been reported from different points of view: expression of a4b7, which is a mucosal homing receptor,<sup>17</sup> VH gene deviation,<sup>6</sup> and IgA production suggesting that lymphoma cells derive from mucosal B cells.<sup>18</sup>

Table 4 Cloning assay of the VH gene of duodenal follicular lymphoma

	CDR2	FR3
Patient no. 12 VH4-61*08	TATATCTATTACAGTGGGAGCACAACACTACAACCCCTCCCTCAAGAGT	CGAGTCACCATATCAGTAGACAGTCCAAAGACAGTCTCCCTGAAGCTGAGCTTCTGACCGCTGCGGACACGCGCCGTATTACTGTGCGGAGA
No. 12	-----G-----T-----	-----A-----C-----
Clone 01	-----G-----T-----	-----A-----C-----
Clone 02	-----G-----T-----	-----A-----C-----
Clone 03	-----G-----T-----	-----A-----C-----
Clone 04	-----G-----T-----	-----A-----C-----
Clone 05	-----G-----T-----	-----A-----C-----
Clone 06	-----G-----T-----	-----A-----C-----
Clone 07	-----G-----T-----	-----A-----C-----
Clone 08	-----G-----T-----	-----A-----C-----
Clone 09	-----G-----T-----	-----A-----C-----
Patient no. 7 VH4-B*02	AGTATCTATCATAGTGGGAGCAGCTACTACTACAACCCCTCCCTCAAGAGT	CGAGTCACCATATCAGTAGACAGTCCAAAGACAGTCTCCCTGAAGCTGAGCTTCTGACCGCGCAGACGCGCCGTATTACTGTGCGGAGA
No. 7	-----G-----T-----	-----A-----C-----
Clone 01	-----G-----T-----	-----A-----C-----
Clone 02	-----G-----T-----	-----A-----C-----
Clone 03	-----G-----T-----	-----A-----C-----
Clone 04	-----G-----T-----	-----A-----C-----
Clone 05	-----G-----T-----	-----A-----C-----
Clone 06	-----G-----T-----	-----A-----C-----
Clone 07	-----G-----T-----	-----A-----C-----
Clone 08	-----G-----T-----	-----A-----C-----

According to our earlier data, we analyzed eight samples for VH usage, and in this study, we analyzed the other 17 samples for VH usage. Therefore, in the 25 samples, 13 (52%) were VH3, 8 (32%) were VH4, and 4 (16%) were VH5. Phenotypically, IgM  $\beta$  memory B cells resemble marginal zone B cells and are thought to be their circulating counterparts.<sup>19</sup> Tsuiji et al<sup>20</sup> reported IgM  $\beta$  memory B cells more frequently express VH3 family genes than do naive B cells. Noppe et al<sup>21</sup> reported VH usage in nodal follicular lymphoma cases as VH3 70%, VH4 19% and VH1 11%; Bahler et al<sup>22</sup> reported it as VH3 67%, VH4 22% and VH1 8%. From their data, duodenal follicular lymphomas of our series showed a higher usage of VH4 and VH5 than did nodal cases. Moreover, VH4-34 and VH5-51 were detected in three samples each in our study. This must not be coincidental, and selective usage strongly suggests that some antigen-dependent mechanism is involved in tumor development, as in the case of MALT lymphoma, which develops from chronic inflammation such as *Helicobacter pylori*-related gastritis.

CD21 is a complement receptor expressed in B cells and follicular dendritic cells in humans.<sup>23</sup> In nodal follicular lymphoma, follicular dendritic cells were important to the microenvironment in which follicular lymphoma cells grow.<sup>24</sup> As shown in the results, although follicular dendritic cell networks were located at the periphery of neoplastic follicles, the major center part of follicular dendritic cells looked broken except for in two samples; by contrast, all nodal lymphomas showed extensively distributed follicular dendritic cells. The shape of degraded follicular dendritic cells are somewhat similar to the follicular colonization of MALT lymphomas, in which marginal zone B-cell lymphoma cells penetrate the non-neoplastic germinal centers and destroy follicular dendritic cell networks (Figure 4). Patient nos. 6 and 16 of the duodenal series showed nodal-pattern follicular dendritic cell. Interestingly, patient no. 16 was associated with markedly swollen mesenteric lymph nodes. Therefore, duodenal lesions of this case were prominent, but the primary site of this case was not clearly determined. Patient nos. 3 and 11 were clinical stage IV, but showed duodenal-pattern follicular dendritic cell. We believe that these duodenal lymphomas possibly progressed to nodal lymphomas.

AID plays key roles in class switching and somatic hypermutation of heavy chains in germinal-center B cells.<sup>7</sup> In an earlier report, RT-PCR showed that follicular lymphoma cells are positive for AID.<sup>8</sup> We examined the samples immunohistochemically, and found that nodal follicular lymphomas had 20% or more AID-positive cells, in contrast to only a few (0.1%) duodenal follicular lymphoma cells that were AID-positive. Our data indicate that most duodenal follicular lymphomas have somatic and ongoing mutations in spite of the lack of AID

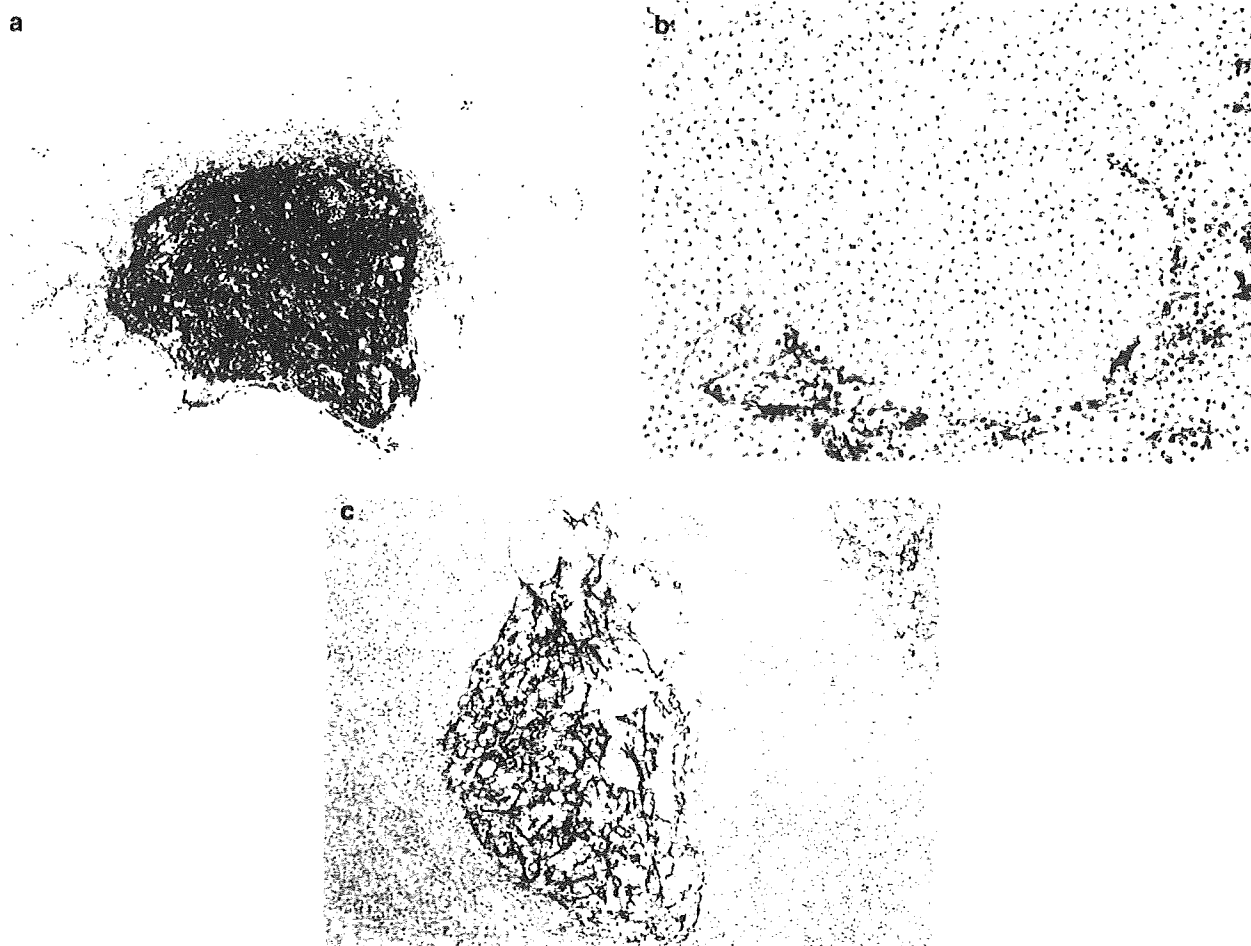


Figure 4 CD21 expression in reactive lymphoid hyperplasia of the duodenum and in MALT lymphoma of the stomach. (a) CD21 expression in reactive lymphoid hyperplasia of the duodenum. Follicular dendritic cell network are present. (b) CD21 expression in MALT lymphoma of the stomach. Follicular dendritic cell network are disrupted (follicular colonization), which is similar to those of duodenal follicular lymphomas. (c) CD21 expression in a non-neoplastic germinal center of a gastric MALT lymphoma. The follicular dendritic cell networks are well preserved.

expression. This sounds contradictory; however, Bombardieri et al<sup>25</sup> reported that neoplastic marginal zone-like B cells are AID-negative but have somatic and ongoing mutations.<sup>26</sup> On the other hand, Smit et al,<sup>27</sup> Pasqualucci et al<sup>28</sup> and Lossos et al<sup>9</sup> reported of lack of correlation between AID expression and intraclonal diversity of VH genes in B-cell non-Hodgkin's lymphomas. And Smit et al<sup>27</sup> mentioned that AID expression at follicular lymphomas were 25%, and intraclonal variation was found in the absence of AID, but they did not explained histology, immunophenotype and stage. IgVH mutations were introduced at a tumor stage when AID enzyme was still expressed. However, from our data, almost all of duodenal follicular lymphoma lacks AID in the protein expression level, and histological grade was 1–2. Moreover, all samples expressed *bcl-6*, which is known to be a target gene for somatic hypermutation in germinal-center B cells.<sup>29</sup> The mechanisms of somatic

and ongoing mutation are not clear. Therefore, in duodenal follicular lymphomas, somatic and ongoing mutation may be independent of AID expression.

Conclusions from our data are as follows: duodenal follicular lymphoma cells showed somatic and ongoing mutations similar to nodal ones, as well as CD10 and *bcl-2* expressions; however, they did not express AID, and the follicular dendritic cell networks essential for 'follicular pattern' lymphomas were severely disrupted, as in the follicular colonization of MALT lymphomas. We also found out that duodenal follicular lymphoma had VH family deviation marked by the presence of very restricted VH4 and VH5 segments, which strongly indicated that the lymphoma cells are derived from B cells reacting with specific antigens. These findings strongly suggested that duodenal follicular lymphoma is distinct from nodal follicular lymphoma, and has more similarity to MALT chronic

inflammation-based lymphomas; these similarities will be very important in considering therapeutic countermeasures against this disease.

## Acknowledgements

This work was supported in part by grants from the Japan Society for the Promotion of Science (JSPS no. 19590348). We thank Ms H Nakamura, Ms M Okabe and Ms M Tokunaka for their technical assistance.

## Conflict of interest

The authors declare no conflict of interest.

## Authorship statement

Takata K, Sato Y, Nakamura N and Yoshino T designed and performed the research. Takata K, Okada H and Tari A prepared specimens and clinical data. Takata K, Kikuti YY, Ichimura K, Tanaka T, Morito T, Tamura M, Oka T and Kondo E analyzed the data. Takata K wrote the paper.

## References

- 1 Yoshino T, Miyake K, Ichimura K, et al. Increased incidence of follicular lymphoma in the duodenum. *Am J Surg Pathol* 2000;24:688–693.
- 2 Shia J, Teruya-Feldstein J, Pan D, et al. Primary follicular lymphoma of the gastrointestinal tract. *Am J Surg Pathol* 2002;26:216–224.
- 3 Kosmas C, Stamatopoulos K, Papadaki T, et al. Somatic hypermutation of immunoglobulin variable region genes: focus on follicular lymphoma and multiple myeloma. *Immunol Rev* 1998;162:281–292.
- 4 Sato Y, Ichimura K, Tanaka T, et al. Duodenal follicular lymphomas share common characteristics with mucosa-associated lymphoid tissue lymphomas. *J Clin Pathol* 2008;61:377–381.
- 5 Mannami T, Yoshino T, Oshima K, et al. Clinical, histopathological, and immunogenetic analysis of ocular adnexal lymphoproliferative disorders: characterization of malt lymphoma and reactive lymphoid hyperplasia. *Mod Pathol* 2001;14:641–649.
- 6 Sato Y, Nakamura N, Nakamura S, et al. Deviated VH4 immunoglobulin gene usage is found among thyroid mucosa-associated lymphoid tissue lymphomas, similar to the usage at other sites, but is not found in thyroid diffuse large B-cell lymphomas. *Mod Pathol* 2006;19:1578–1584.
- 7 Muramatsu M, Kinoshita K, Fagarasan S, et al. Class switch recombination and hypermutation require activation-induced cytidine deaminase (AID), a potential RNA editing enzyme. *Cell* 2000;102:553–563.
- 8 Hardianti MS, Tatsumi E, Syampurnawati M, et al. Activation-induced cytidine deaminase expression in follicular lymphoma: association between AID expression and ongoing mutation in FL. *Leukemia* 2004;18:826–831.
- 9 Lossos IS, Levy R, Alizadeh AA. AID is expressed in germinal center B-cell-like and activated B-cell-like diffuse large-cell lymphomas and is not correlated with intraclonal heterogeneity. *Leukemia* 2004;18:1775–1779.
- 10 Joseph DK, Dan J, Marwan AY, et al. Bone marrow involvement in patients with nodular lymphocyte predominant Hodgkin lymphoma. *Am J Surg Pathol* 2004;28:489–495.
- 11 Nakamura N, Kuze T, Hashimoto Y, et al. Analysis of the immunoglobulin heavy chain gene variable region of CD5-positive and -negative diffuse large B cell lymphoma. *Leukemia* 2001;15:452–457.
- 12 Nakamura N, Hashimoto Y, Kuze T, et al. Analysis of the immunoglobulin heavy chain gene variable region of CD5-positive diffuse large B cell lymphoma. *Lab Invest* 1999;79:925–933.
- 13 Takada S, Yoshino T, Taniwaki M, et al. Involvement of the chromosomal translocation t(11;18) in some mucosa-associated lymphoid tissue lymphomas and diffuse large B cell lymphomas of the ocular Adnexa Evidence from multiplex reverse transcriptase-polymerase chain reaction and fluorescence in situ hybridization on using formalin-fixed, paraffin-embedded specimens. *Mod Pathol* 2003;16:445–452.
- 14 Rohatiner A, d'Amore F, Coiffier B, et al. Report on a workshop convened to discuss the pathological and staging classifications of gastrointestinal tract lymphoma. *Ann Oncol* 1994;5:397–400.
- 15 Bagdi E, Krenacs L, Krenacs T, et al. Follicular dendritic cells in reactive and neoplastic lymphoid tissues: a reevaluation of staining patterns of CD21, CD23, and CD35 antibodies in paraffin sections after wet heat-induced epitope retrieval. *Appl Immunohistochem Mol Morphol* 2001;9:117–124.
- 16 Sweldlow SH, Campo E, Harris NL, et al., editor WHO Classifications of Tumours of Haematopoietic and Lymphoid Tissues, 4th edn, IARC Lyon, 2008; 220–226p.
- 17 Liu YX, Yoshino T, Ohara N, et al. Loss of expression of alpha4beta7 integrin and L-selectin is associated with high-grade progression of low-grade MALT lymphoma. *Mod Pathol* 2001;14:798–805.
- 18 Bende RJ, Smit LA, Bossenbroek JG, et al. Primary follicular lymphoma of the small intestine: alpha4beta7 expression and immunoglobulin configuration suggest an origin from local antigen-experienced B cells. *Am J Pathol* 2003;162:105–113.
- 19 Weller S, Braun MC, Tan BK, et al. Human blood IgM 'memory' B cells are circulating splenic marginal zone B cells harboring a pre-diversified immunoglobulin repertoire. *Blood* 2004;104:3647–3654.
- 20 Tsuiji M, Yurasov S, Velinzon K, et al. A checkpoint for autoreactivity in human IgM+ memory B cell development. *J Exp Med* 2006;203:393–400.
- 21 Noppe SM, Heirman C, Bakkus MHC, et al. The genetic variability of the VH genes in follicular lymphoma: the impact of the hypermutation mechanism. *Br J Haematol* 1999;107:625–640.
- 22 David WB, Michael JC, Sarah H, et al. IgVH gene expression among human follicular lymphomas. *Blood* 1991;78:1561–1568.
- 23 Rosendaal R, Carroli MC. Complement receptors CD21 and CD35 in humoral immunity. *Immunol Rev* 2007;219:157–166.
- 24 Kagami Y, Jung J, Choi YS, et al. Establishment of a follicular lymphoma cell line (FLK-1) dependent on follicular dendritic cell-like cell line HK. *Leukemia* 2001;15:148–156.

- 25 Bombardieri M, Barone F, Humby F, et al. Activation-induced cytidine deaminase expression in follicular dendritic cell networks and interfollicular large B cells supports functionality of ectopic lymphoid neogenesis in autoimmune sialoadenitis and MALT lymphoma in Sjogren's syndrome. *J Immunol* 2007;179:4929–4938.
- 26 Behler DW, Miklos JA, Swerdlow SH. Ongoing Ig gene hypermutation in salivary gland mucosa-associated lymphoid tissue-type lymphomas. *Blood* 1997;89:3335–3344.
- 27 Smit LA, Bende RJ, Aten J, et al. Expression of activation-induced cytidine deaminase is confined to B-cell Non-Hodgkin's lymphomas of germinal-center phenotype. *Cancer Res* 2003;15:3894–3898.
- 28 Pasqualucci L, Guglielmino R, Houldsworth J, et al. Expression of the AID protein in normal and neoplastic B cells. *Blood* 2004;104:3318–3325.
- 29 Klein UIF, Dalla-Favera R. Germinal centers: role in B-cell physiology and malignancy. *Nat Rev Immunol* 2008;8:22–33.

## LETTERS

## Frequent inactivation of A20 in B-cell lymphomas

Motohiro Kato<sup>1,2</sup>, Masashi Sanada<sup>1,5</sup>, Itaru Kato<sup>6</sup>, Yasuharu Sato<sup>7</sup>, Junko Takita<sup>1,2,3</sup>, Kengo Takeuchi<sup>8</sup>, Akira Niwa<sup>6</sup>, Yuyan Chen<sup>1,2</sup>, Kumi Nakazaki<sup>1,4,5</sup>, Junko Nomoto<sup>9</sup>, Yoshitaka Asakura<sup>9</sup>, Satsuki Muto<sup>1</sup>, Azusa Tamura<sup>1</sup>, Mitsuru Iio<sup>1</sup>, Yoshiaki Akatsuka<sup>11</sup>, Yasuhide Hayashi<sup>12</sup>, Hiraku Mori<sup>13</sup>, Takashi Igarashi<sup>2</sup>, Mineo Kurokawa<sup>4</sup>, Shigeru Chiba<sup>3</sup>, Shigeo Mori<sup>14</sup>, Yuichi Ishikawa<sup>8</sup>, Koji Okamoto<sup>10</sup>, Kensei Tobinai<sup>9</sup>, Hitoshi Nakagama<sup>10</sup>, Tatsutoshi Nakahata<sup>6</sup>, Tadashi Yoshino<sup>7</sup>, Yukio Kobayashi<sup>9</sup> & Seishi Ogawa<sup>1,5</sup>

A20 is a negative regulator of the NF- $\kappa$ B pathway and was initially identified as being rapidly induced after tumour-necrosis factor- $\alpha$  stimulation<sup>1</sup>. It has a pivotal role in regulation of the immune response and prevents excessive activation of NF- $\kappa$ B in response to a variety of external stimuli<sup>2-7</sup>; recent genetic studies have disclosed putative associations of polymorphic A20 (also called *TNFAIP3*) alleles with autoimmune disease risk<sup>8,9</sup>. However, the involvement of A20 in the development of human cancers is unknown. Here we show, using a genome-wide analysis of genetic lesions in 238 B-cell lymphomas, that A20 is a common genetic target in B-lineage lymphomas. A20 is frequently inactivated by somatic mutations and/or deletions in mucosa-associated tissue lymphoma (18 out of 87; 21.8%) and Hodgkin's lymphoma of nodular sclerosis histology (5 out of 15; 33.3%), and, to a lesser extent, in other B-lineage lymphomas. When re-expressed in a lymphoma-derived cell line with no functional A20 alleles, wild-type A20, but not mutant A20, resulted in suppression of cell growth and induction of apoptosis, accompanied by downregulation of NF- $\kappa$ B activation. The A20-deficient cells stably generated tumours in immunodeficient mice, whereas the tumorigenicity was effectively suppressed by re-expression of A20. In A20-deficient cells, suppression of both cell growth and NF- $\kappa$ B activity due to re-expression of A20 depended, at least partly, on cell-surface-receptor signalling, including the tumour-necrosis factor receptor. Considering the physiological function of A20 in the negative modulation of NF- $\kappa$ B activation induced by multiple upstream stimuli, our findings indicate that uncontrolled signalling of NF- $\kappa$ B caused by loss of A20 function is involved in the pathogenesis of subsets of B-lineage lymphomas.

Malignant lymphomas of B-cell lineages are mature lymphoid neoplasms that arise from various lymphoid tissues<sup>10,11</sup>. To obtain a comprehensive registry of genetic lesions in B-lineage lymphomas, we performed a single nucleotide polymorphism (SNP) array analysis of 238 primary B-cell lymphoma specimens of different histologies, including 64 samples of diffuse large B-cell lymphomas (DLBCLs), 52 follicular lymphomas, 35 mantle cell lymphomas (MCLs), and 87 mucosa-associated tissue (MALT) lymphomas (Supplementary Table 1). Three Hodgkin's-lymphoma-derived cell lines were also analysed. Interrogating more than 250,000 SNP sites, this platform permitted the identification of copy number changes at an average resolution of less than 12 kilobases (kb). The use of large numbers of

SNP-specific probes is a unique feature of this platform, and combined with the CNAG/AsCNAR software, enabled accurate determination of 'allele-specific' copy numbers, and thus allowed for sensitive detection of loss of heterozygosity (LOH) even without apparent copy-number reduction, in the presence of up to 70–80% normal cell contamination<sup>12,13</sup>.

Lymphoma genomes underwent a wide range of genetic changes, including numerical chromosomal abnormalities and segmental gains and losses of chromosomal material (Supplementary Fig. 1), as well as copy-number-neutral LOH, or uniparental disomy (Supplementary Fig. 2). Each histology type had a unique genomic signature, indicating a distinctive underlying molecular pathogenesis for different histology types (Fig. 1a and Supplementary Fig. 3). On the basis of the genomic signatures, the initial pathological diagnosis of MCL was re-evaluated and corrected to DLBCL in two cases. Although most copy number changes involved large chromosomal segments, a number of regions showed focal gains and deletions, accelerating identification of their candidate gene targets. After excluding known copy number variations, we identified 46 loci showing focal gains (19 loci) or deletions (27 loci) (Supplementary Tables 2 and 3 and Supplementary Fig. 4).

Genetic lesions on the NF- $\kappa$ B pathway were common in B-cell lymphomas and found in approximately 40% of the cases (Supplementary Table 1), underpinning the importance of aberrant NF- $\kappa$ B activation in lymphomagenesis<sup>11,14</sup> in a genome-wide fashion. They included focal gain/amplification at the *REL* locus (16.4%) (Fig. 1b) and *TRAF6* locus (5.9%), as well as focal deletions at the *PTEN* locus (5.5%) (Supplementary Figs 1 and 4). However, the most striking finding was the common deletion at 6q23.3 involving a 143-kb segment. It exclusively contained the A20 gene (also called *TNFAIP3*), a negative regulator of NF- $\kappa$ B activation<sup>3-7,15</sup> (Fig. 1b), which was previously reported as a candidate target of 6q23 deletions in ocular lymphoma<sup>16</sup>. LOH involving the A20 locus was found in 50 cases, of which 12 showed homozygous deletions as determined by the loss of both alleles in an allele-specific copy number analysis (Fig. 1b, Table 1 and Supplementary Table 4). On the basis of this finding, we searched for possible tumour-specific mutations of A20 by genomic DNA sequencing of entire coding exons of the gene in the same series of lymphoma samples (Supplementary Fig. 5). Because two out of the three Hodgkin's-lymphoma-derived cell lines had biallelic A20 deletions/mutations (Supplementary Fig. 6), 24 primary samples from Hodgkin's lymphoma were also analysed for mutations, where

<sup>1</sup>Cancer Genomics Project, Department of <sup>2</sup>Pediatrics, <sup>3</sup>Cell Therapy and Transplantation Medicine, and <sup>4</sup>Hematology and Oncology, Graduate School of Medicine, University of Tokyo, 7-3-1 Hongo, Bunkyo-ku, Tokyo 113-8655, Japan. <sup>5</sup>Core Research for Evolutional Science and Technology, Japan Science and Technology Agency, 4-1-8, Honcho, Kawaguchi-shi, Saitama 332-0012, Japan. <sup>6</sup>Department of Pediatrics, Graduate School of Medicine, Kyoto University, 54 Kawahara-cho, Shogoin, Sakyo-ku, Kyoto 606-8507, Japan. <sup>7</sup>Department of Pathology, Okayama University Graduate School of Medicine, Dentistry and Pharmaceutical Sciences, 2-5-1 Shikata-cho, Kita-ku, Okayama 700-8558, Japan. <sup>8</sup>Division of Pathology, The Cancer Institute of Japanese Foundation for Cancer Research, Japan, 3-10-6 Ariake, Koto-ku, Tokyo 135-8550, Japan. <sup>9</sup>Hematology Division, Hospital, and <sup>10</sup>Early Oncogenesis Research Project, Research Institute, National Cancer Center, 5-1-1 Tsukiji, Chuo-ku, Tokyo 104-0045, Japan. <sup>11</sup>Division of Immunology, Aichi Cancer Center Research Institute, 1-1 Kanokoden, Chikusa-ku, Nagoya 464-8681, Japan. <sup>12</sup>Gunma Children's Medical Center, 779 Shimohakoda, Hokkitsu-machi, Shibukawa 377-8577, Japan. <sup>13</sup>Division of Hematology, Internal Medicine, Showa University Fujigaoka Hospital, 1-30, Fujigaoka, Aoba-ku, Yokohama-shi, Kanagawa 227-8501, Japan. <sup>14</sup>Department of Pathology, Teikyo University School of Medicine, 2-11-1 Kaga, Itabashi-ku, Tokyo 173-8605, Japan.



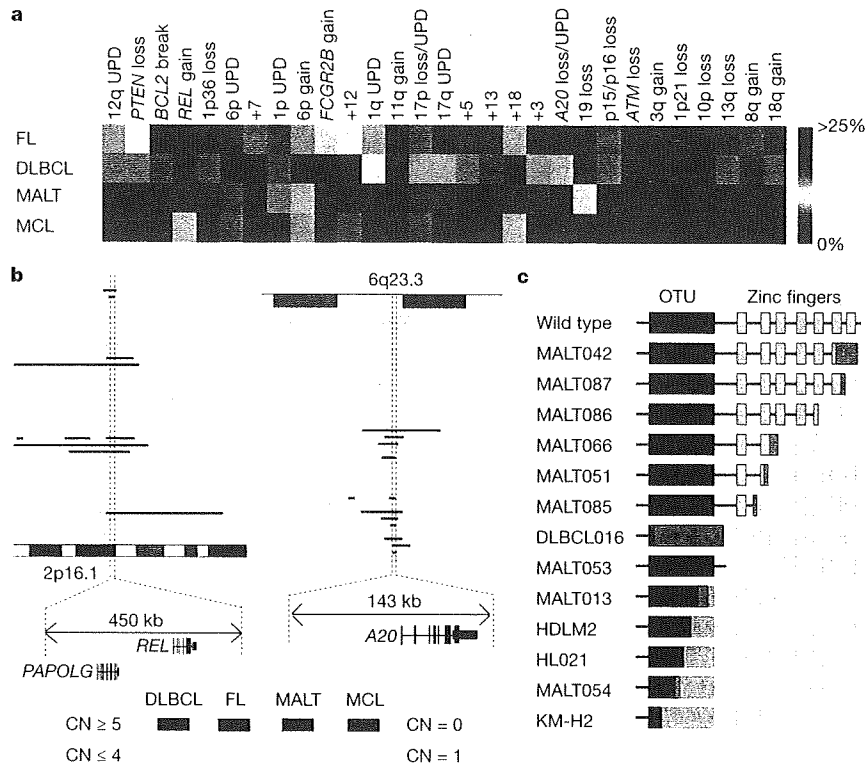


**Figure 1 | Genomic signatures of different B-cell lymphomas and common genetic lesions at 2p16-15 and 6q23.3 involving NF-κB pathway genes.** **a**, Twenty-nine genetic lesions were found in more than 10% in at least one histology and used for clustering four distinct histology types of B-lineage lymphomas. The frequency of each genetic lesion in each histology type is colour-coded. FL, follicular lymphoma; UPD, uniparental disomy. **b**, Recurrent genetic changes are depicted based on CNAG output of the SNP array analysis of 238 B-lineage lymphoma samples, which include gains at the REL locus on 2p16-15 (left panel) and the A20 locus on 6q23.3 (right

panel). Regions showing copy number gain or loss are indicated by horizontal lines. Four histology types are indicated by different colours, where high-grade amplifications and homozygous deletions are shown by darker shades to discriminate from simple gains (copy number ≤4) and losses (copy number = 1) (lighter shades). **c**, Point mutations and small nucleotide insertions and deletions in the A20 (TNFAIP3) gene caused premature truncation of A20 in most cases. Altered amino acids caused by frame shifts are indicated by green bars.

genomic DNA was extracted from 150 microdissected CD30-positive tumour cells (Reed–Sternberg cells) for each sample. A20 mutations were found in 18 out of 265 lymphoma samples (6.8%) (Table 1), among which 13 mutations, including nonsense mutations (3 cases), frame-shift insertions/deletions (9 cases), and a splicing donor site mutation (1 case) were thought to result in premature termination of translation (Fig. 1c). Four missense mutations and one intronic mutation were identified in five microdissected Hodgkin’s lymphoma samples. They were not found in the surrounding normal tissues, and thus, were considered as tumour-specific somatic changes.

In total, biallelic A20 lesions were found in 31 out of 265 lymphoma samples including 3 Hodgkin’s lymphoma cell lines. Quantitative analysis of SNP array data suggested that these A20 lesions were present in the major tumour fraction within the samples (Supplementary Fig. 7). Inactivation of A20 was most frequent in MALT lymphoma (18 out of 87) and Hodgkin’s lymphoma (7 out of 27), although it was also found in DLBCL (5 out of 64) and follicular lymphoma (1 out of 52) at lower frequencies. In MALT lymphoma, biallelic A20 lesions were confirmed in 18 out of 24 cases (75.0%) with LOH involving the 6q23.3 segment (Supplementary Fig. 8). Considering the limitation in detecting very small homozygous deletions, A20 was thought to be the target of 6q23 LOH in MALT lymphoma. On the other hand, the 6q23 LOHs in other histology types tended to be extended into more centromeric regions and less frequently accompanied biallelic A20 lesions (Supplementary Fig. 8 and Supplementary Table 4), indicating that they might be more

heterogeneous with regard to their gene targets. We were unable to analyse Hodgkin’s lymphoma samples using SNP arrays owing to insufficient genomic DNA obtained from microdissected samples, and were likely to underestimate the frequency of A20 inactivation in Hodgkin’s lymphoma because we might fail to detect a substantial proportion of cases with homozygous deletions, which explained 50% (12 out of 24) of A20 inactivation in other histology types. A20 mutations in Hodgkin’s lymphoma were exclusively found in nodular sclerosis classical Hodgkin’s lymphoma (5 out of 15) but not in other histology types (0 out of 9), although the possible association requires further confirmation in additional cases.

A20 is a key regulator of NF-κB signalling, negatively modulating NF-κB activation through a wide variety of cell surface receptors and viral proteins, including tumour-necrosis factor (TNF) receptors, toll-like receptors, CD40, as well as Epstein–Barr-virus-associated LMP1 protein<sup>2,5,17,18</sup>. To investigate the role of A20 inactivation in lymphomagenesis, we re-expressed wild-type A20 under a Tet-inducible promoter in a lymphoma-derived cell line (KM-H2) that had no functional A20 alleles (Supplementary Fig. 6), and examined the effect of A20 re-expression on cell proliferation, survival and downstream NF-κB signalling pathways. As shown in Fig. 2a–c and Supplementary Fig. 9, re-expression of wild-type A20 resulted in the suppression of cell proliferation and enhanced apoptosis, and in the concomitant accumulation of IκBβ and IκBe, and downregulation of NF-κB activity. In contrast, re-expression of two lymphoma-derived A20 mutants, A20<sup>532Stop</sup> or A20<sup>750Stop</sup>, failed to show growth suppression, induction of apoptosis, accumulation of IκBβ and IκBe or downregulation of

**Table 1 | Inactivation of A20 in B-lineage lymphomas**

Histology	Tissue	Sample	Allele	Uniparental disomy	Exon	Mutation	Biallelic inactivation
DLBCL	Lymph node	DLBCL008	-/-	No	-	-	5 out of 64 (7.8%)
	Lymph node	DLBCL016	+/-	No	Ex2	329insA	
	Lymph node	DLBCL022	-/-	No	-	-	
	Lymph node	DLBCL028	-/-	Yes	-	-	
	Lymph node	MCL008*	-/-	Yes	-	-	
Follicular lymphoma	Lymph node	FL024	-/-	No	-	-	1 out of 52 (1.9%)
MCL							0 out of 35 (0%)
MALT							18 out of 87 (21.8%)
Stomach							3 out of 23 (13.0%)
	Gastric mucosa	MALT013	+/+	Yes	Ex5	705insG	
	Gastric mucosa	MALT014	+/+	Yes	Ex3	Ex3 donor site>A	
	Gastric mucosa	MALT036	+/-	No	Ex7	delintron6-Ex7†	
Eye							13 out of 43 (30.2%)
	Ocular adnexa	MALT008	-/-	No	-	-	
	Ocular adnexa	MALT017	-/-	No	-	-	
	Ocular adnexa	MALT051	+/-	No	Ex7	1943delTG	
	Ocular adnexa	MALT053	+/+	Yes	Ex6	1016G>A(stop)	
	Ocular adnexa	MALT054	+/-	No	Ex3	502delTC	
	Ocular adnexa	MALT055	-/-	No	-	-	
	Ocular adnexa	MALT066	+/-	No	Ex7	1581insA	
	Ocular adnexa	MALT067	-/-	No	-	-	
	Ocular adnexa	MALT082	-/-	Yes	-	-	
	Ocular adnexa	MALT084	-/-	Yes	-	-	
	Ocular adnexa	MALT085	+/+	Yes	Ex7	1435insG	
	Ocular adnexa	MALT086	+/+	Yes	Ex6	878C>T(stop)	
Ocular adnexa	MALT087	+/+	Yes	Ex9	2304delGG		
Lung	Lung	MALT042	-/-	No	-	-	2 out of 12 (16.7%)
	Lung	MALT047	+/+	Yes	Ex9	2281insT	
Other‡							0 out of 9 (0%)
Hodgkin's lymphoma							7 out of 27 (26.0%)
NSHL	Lymph node	HL10	ND	ND	Ex7	1777G>A(V571I)	
NSHL	Lymph node	HL12	ND	ND	Ex7	1156A>G(R364G)	
NSHL	Lymph node	HL21	ND	ND	Ex4	569G>A(stop)	
NSHL	Lymph node	HL24	ND	ND	Ex3	1487C>A(T474N)	
NSHL	Lymph node	HL23	ND	ND	-	Intron 3§	
	Cell line	KM-H2	-/-	No	-	-	
	Cell line	HDLM2	+/-	No	Ex4	616ins29bp	
<b>Total</b>							<b>31 out of 265 (11.7%)</b>

DLBCL, diffuse large B-cell lymphoma; MALT, MALT lymphoma; MCL, mantle cell lymphoma; ND, not determined because SNP array analysis was not performed; NSHL, nodular sclerosis classical Hodgkin's lymphoma.

\* Diagnosis was changed based on the genomic data, which was confirmed by re-examination of pathology.

† Deletion including the boundary of intron 6 and exon 7 (see also Supplementary Fig. 5b).

‡ Including 1 parotid gland, 1 salivary gland, 2 colon and 5 thyroid cases.

§ Insertion of CTC at -19 bases from the beginning of exon 3.

|| Insertion of TGGCTTCCACAGACACACCCATGGCCCGA.

NF- $\kappa$ B activity (Fig. 2a–c), indicating that these were actually loss-of-function mutations. To investigate the role of A20 inactivation in lymphomagenesis *in vivo*, A20- and mock-transduced KM-H2 cells were transplanted in NOD/SCID/ $\gamma_c^{\text{null}}$  (NOG) mice<sup>19</sup>, and their tumour formation status was examined for 5 weeks with or without induction of wild-type A20 by tetracycline administration. As shown in Fig. 2d, mock-transduced cells developed tumours at the injected sites, whereas the *Tet*-inducible A20-transduced cells generated tumours only in the absence of A20 induction (Supplementary Table 5), further supporting the tumour suppressor role of A20 in lymphoma development.

Given the mode of negative regulation of NF- $\kappa$ B signalling, we next investigated the origins of NF- $\kappa$ B activity that was deregulated by A20 loss in KM-H2 cells. The conditioned medium prepared from a 48-h serum-free KM-H2 culture had increased NF- $\kappa$ B upregulatory activity compared with fresh serum-free medium, which was inhibited by re-expression of A20 (Fig. 3a). KM-H2 cells secreted two known ligands for TNF receptor—TNF- $\alpha$  and lymphotoxin- $\alpha$  (Supplementary Fig. 10)<sup>20</sup>—and adding neutralizing antibodies against these cytokines into cultures significantly suppressed their cell growth and NF- $\kappa$ B activity without affecting the levels of their overall suppression after A20

induction (Fig. 3b, d). In addition, recombinant TNF- $\alpha$  and/or lymphotoxin- $\alpha$  added to fresh serum-free medium promoted cell growth and NF- $\kappa$ B activation in KM-H2 culture, which were again suppressed by re-expression of A20 (Fig. 3c, e). Although our data in Fig. 3 also show the presence of factors other than TNF- $\alpha$  and lymphotoxin- $\alpha$  in the KM-H2-conditioned medium—as well as some intrinsic pathways in the cell (Fig. 3a)—that were responsible for the A20-dependent NF- $\kappa$ B activation, these results indicate that both cell growth and NF- $\kappa$ B activity that were upregulated by A20 inactivation depend at least partly on the upstream stimuli that evoked the NF- $\kappa$ B-activating signals.

Aberrant activation of the NF- $\kappa$ B pathway is a hallmark of several subtypes of B-lineage lymphomas, including Hodgkin's lymphoma, MALT lymphoma, and a subset of DLBCL, as well as other lymphoid neoplasms<sup>11,14</sup>, where a number of genetic alterations of NF- $\kappa$ B signalling pathway genes<sup>21–25</sup>, as well as some viral proteins<sup>26,27</sup>, have been implicated in the aberrant activation of the NF- $\kappa$ B pathway<sup>14</sup>. Thus, frequent inactivation of A20 in Hodgkin's lymphoma and MALT and other lymphomas provides a novel insight into the molecular pathogenesis of these subtypes of B-lineage lymphomas through deregulated NF- $\kappa$ B activation. Because A20 provides a

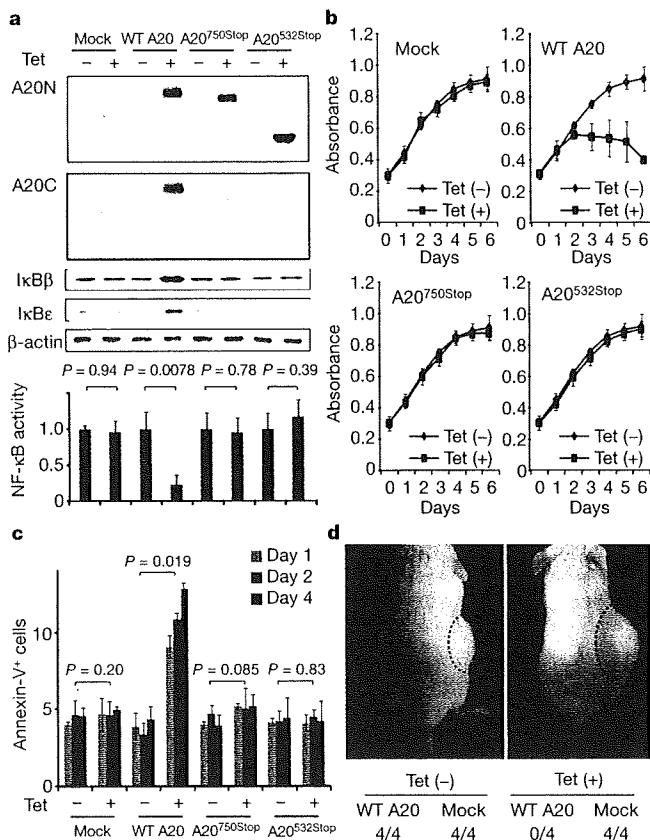


**Figure 2 | Effects of wild-type and mutant A20 re-expressed in a lymphoma cell line that lacks the normal A20 gene.** **a**, Western blot analyses of wild-type (WT) and mutant (A20<sup>532Stop</sup> and A20<sup>750Stop</sup>) A20, as well as IκBβ and IκBε, in KM-H2 cells, in the presence or absence of tetracycline treatment (top panels). A20N and A20C are polyclonal antisera raised against N-terminal and C-terminal A20 peptides, respectively. β-actin blots are provided as a control. NF-κB activities are expressed as mean absorbance ± s.d. (*n* = 6) in luciferase assays (bottom panel). **b**, Proliferation of KM-H2 cells stably transduced with plasmids for mock and Tet-inducible wild-type A20, A20<sup>532Stop</sup> and A20<sup>750Stop</sup> was measured using a cell counting kit in the presence (red lines) or absence (blue lines) of tetracycline. Mean absorbance ± s.d. (*n* = 5) is plotted. **c**, The fractions of Annexin-V-positive KM-H2 cells transduced with various Tet-inducible A20 constructs were measured by flow cytometry after tetracycline treatment and the mean values (± s.d., *n* = 3) are plotted. **d**, *In vivo* tumorigenicity was assayed by inoculating 7 × 10<sup>6</sup> KM-H2 cells transduced with mock or Tet-inducible wild-type A20 in NOG mice, with (right panel) or without (left panel) tetracycline administration.

negative feedback mechanism in the regulation of NF-κB signalling pathways upon a variety of stimuli, aberrant activation of NF-κB will be a logical consequence of A20 inactivation. However, there is also the possibility that the aberrant NF-κB activity of A20-inactivated lymphoma cells is derived from upstream stimuli, which may be from the cellular environment. In this context, it is intriguing that MALT lymphoma usually arises at the site of chronic inflammation caused by infection or autoimmune disorders and may show spontaneous regression after eradication of infectious organisms<sup>28</sup>; furthermore, Hodgkin's lymphoma frequently shows deregulated cytokine production from Reed–Sternberg cells and/or surrounding reactive cells<sup>29</sup>. Detailed characterization of the NF-κB pathway regulated by A20 in both normal and neoplastic B lymphocytes will promote our understanding of the precise roles of A20 inactivation in the pathogenesis of these lymphoma types. Our finding underscores the importance of genome-wide approaches in the identification of genetic targets in human cancers.

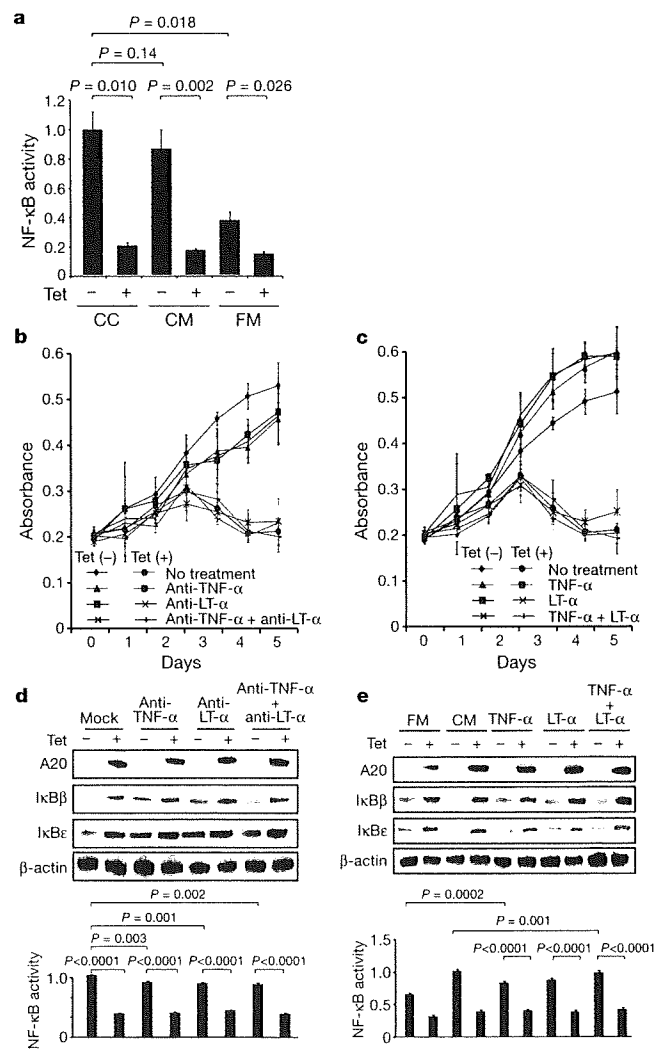


**Figure 3 | Tumour suppressor role of A20 under external stimuli.** **a**, NF-κB activity in KM-H2 cells was measured 30 min after cells were inoculated into fresh medium (FM) or KM-H2-conditioned medium (CM) obtained from the 48-h culture of KM-H2, and was compared with the activity after 48 h continuous culture of KM-H2 (CC). A20 was induced 12 h before inoculation in Tet (+) groups. **b**, **c**, Effects of neutralizing antibodies against TNF-α and lymphotoxin-α (LTα) (**b**) and of recombinant TNF-α and LT-α added to the culture (**c**) on cell growth were evaluated in the presence (Tet (+)) or absence (Tet (-)) of A20 induction. Cell numbers were measured using a cell counting kit and are plotted as their mean absorbance ± s.d. (*n* = 6). **d**, **e**, Effects of the neutralizing antibodies (**d**) and the recombinant cytokines added to the culture (**e**) on NF-κB activities and the levels of IκBβ and IκBε after 48 h culture with (Tet (+)) or without (Tet (-)) tetracycline treatment. NF-κB activities are expressed as mean absorbance ± s.d. (*n* = 6) in luciferase assays.

**METHODS SUMMARY**

Genomic DNA from 238 patients with non-Hodgkin's lymphoma and three Hodgkin's-lymphoma-derived cell lines was analysed using GeneChip SNP genotyping microarrays (Affymetrix). This study was approved by the ethics boards of the University of Tokyo, National Cancer Institute Hospital, Okayama University, and the Cancer Institute of the Japanese Foundation of Cancer Research. After appropriate normalization of mean array intensities, signal ratios between tumours and anonymous normal references were calculated in an allele-specific manner, and allele-specific copy numbers were inferred from the observed signal ratios based on the hidden Markov model using CNAG/AsCNAR software (<http://www.genome.umin.jp>). A20 mutations were examined by directly sequencing genomic DNA using a set of primers (Supplementary Table 6). Full-length cDNAs of wild-type and mutant A20 were introduced into a

lentivirus vector, pLenti4/TO/V5-DEST (Invitrogen), with a *Tet*-inducible promoter. Viral stocks were prepared by transfecting the vector plasmids into 293FT cells (Invitrogen) using the calcium phosphate method and then infected to the KM-H2 cell line. Proliferation of KM-H2 cells was measured using a Cell Counting Kit (Dojindo). Western blot analyses and luciferase assays were performed as previously described. NF- $\kappa$ B activity was measured by luciferase assays in KM-H2 cells stably transduced with a reporter plasmid having an NF- $\kappa$ B response element, pGL4.32 (Promega). Apoptosis of KM-H2 upon A20 induction was evaluated by counting Annexin-V-positive cells by flow cytometry. For *in vivo* tumorigenicity assays,  $7 \times 10^6$  KM-H2 cells were transduced with the *Tet*-inducible A20 gene and those with a mock vector were inoculated on the contralateral sides in eight NOG mice<sup>19</sup> and examined for their tumour formation with ( $n = 4$ ) or without ( $n = 4$ ) tetracycline administration. Full copy number data of the 238 lymphoma samples will be accessible from the Gene Expression Omnibus (GEO, <http://ncbi.nlm.nih.gov/geo/>) with the accession number GSE12906.

**Full Methods** and any associated references are available in the online version of the paper at [www.nature.com/nature](http://www.nature.com/nature).

Received 17 September 2008; accepted 3 March 2009.

Published online 3 May 2009.

- Dixit, V. M. *et al.* Tumor necrosis factor- $\alpha$  induction of novel gene products in human endothelial cells including a macrophage-specific chemotaxin. *J. Biol. Chem.* **265**, 2973–2978 (1990).
- Song, H. Y., Rothe, M. & Goeddel, D. V. The tumor necrosis factor-inducible zinc finger protein A20 interacts with TRAF1/TRAF2 and inhibits NF- $\kappa$ B activation. *Proc. Natl Acad. Sci. USA* **93**, 6721–6725 (1996).
- Lee, E. G. *et al.* Failure to regulate TNF-induced NF- $\kappa$ B and cell death responses in A20-deficient mice. *Science* **289**, 2350–2354 (2000).
- Boone, D. L. *et al.* The ubiquitin-modifying enzyme A20 is required for termination of Toll-like receptor responses. *Nature Immunol.* **5**, 1052–1060 (2004).
- Wang, Y. Y., Li, L., Han, K. J., Zhai, Z. & Shu, H. B. A20 is a potent inhibitor of TLR3- and Sendai virus-induced activation of NF- $\kappa$ B and ISRE and IFN- $\beta$  promoter. *FEBS Lett.* **576**, 86–90 (2004).
- Wertz, I. E. *et al.* De-ubiquitination and ubiquitin ligase domains of A20 downregulate NF- $\kappa$ B signalling. *Nature* **430**, 694–699 (2004).
- Heyninck, K. & Beyaert, R. A20 inhibits NF- $\kappa$ B activation by dual ubiquitin-editing functions. *Trends Biochem. Sci.* **30**, 1–4 (2005).
- Graham, R. R. *et al.* Genetic variants near *TNFAIP3* on 6q23 are associated with systemic lupus erythematosus. *Nature Genet.* **40**, 1059–1061 (2008).
- Musone, S. L. *et al.* Multiple polymorphisms in the *TNFAIP3* region are independently associated with systemic lupus erythematosus. *Nature Genet.* **40**, 1062–1064 (2008).
- Jaffe, E. S., Harris, N. L., Stein, H. & Vardiman, J. W. *World Health Organization Classification of Tumours. Pathology and Genetics of Tumours of Hematopoietic and Lymphoid Tissues* (IARC Press, 2001).
- Klein, U. & Dalla-Favera, R. Germinal centres: role in B-cell physiology and malignancy. *Nature Rev. Immunol.* **8**, 22–33 (2008).
- Nannya, Y. *et al.* A robust algorithm for copy number detection using high-density oligonucleotide single nucleotide polymorphism genotyping arrays. *Cancer Res.* **65**, 6071–6079 (2005).
- Yamamoto, G. *et al.* Highly sensitive method for genomewide detection of allelic composition in nonpaired, primary tumor specimens by use of affymetrix single-nucleotide-polymorphism genotyping microarrays. *Am. J. Hum. Genet.* **81**, 114–126 (2007).
- Jost, P. J. & Ruland, J. Aberrant NF- $\kappa$ B signaling in lymphoma: mechanisms, consequences, and therapeutic implications. *Blood* **109**, 2700–2707 (2007).
- Durkop, H., Hirsch, B., Hahn, C., Foss, H. D. & Stein, H. Differential expression and function of A20 and TRAF1 in Hodgkin lymphoma and anaplastic large cell lymphoma and their induction by CD30 stimulation. *J. Pathol.* **200**, 229–239 (2003).
- Honma, K. *et al.* *TNFAIP3* is the target gene of chromosome band 6q23.3-q24.1 loss in ocular adnexal marginal zone B cell lymphoma. *Genes Chromosom. Cancer* **47**, 1–7 (2008).
- Sarma, V. *et al.* Activation of the B-cell surface receptor CD40 induces A20, a novel zinc finger protein that inhibits apoptosis. *J. Biol. Chem.* **270**, 12343–12346 (1995).
- Fries, K. L., Miller, W. E. & Raab-Traub, N. The A20 protein interacts with the Epstein-Barr virus latent membrane protein 1 (LMP1) and alters the LMP1/TRAF1/TRADD complex. *Virology* **264**, 159–166 (1999).
- Hiramatsu, H. *et al.* Complete reconstitution of human lymphocytes from cord blood CD34<sup>+</sup> cells using the NOD/SCID/ $\gamma^{\text{null}}$  mice model. *Blood* **102**, 873–880 (2003).
- Hsu, P. L. & Hsu, S. M. Production of tumor necrosis factor- $\alpha$  and lymphotoxin by cells of Hodgkin's neoplastic cell lines HDLM-1 and KM-H2. *Am. J. Pathol.* **135**, 735–745 (1989).
- Dierlamm, J. *et al.* The apoptosis inhibitor gene *API2* and a novel 18q gene, *MLT*, are recurrently rearranged in the t(11;18)(q21;q21) associated with mucosa-associated lymphoid tissue lymphomas. *Blood* **93**, 3601–3609 (1999).
- Willis, T. G. *et al.* Bcl10 is involved in t(1;14)(p22;q32) of MALT B cell lymphoma and mutated in multiple tumor types. *Cell* **96**, 35–45 (1999).
- Joos, S. *et al.* Classical Hodgkin lymphoma is characterized by recurrent copy number gains of the short arm of chromosome 2. *Blood* **99**, 1381–1387 (2002).
- Martin-Subero, J. I. *et al.* Recurrent involvement of the *REL* and *BCL11A* loci in classical Hodgkin lymphoma. *Blood* **99**, 1474–1477 (2002).
- Lenz, G. *et al.* Oncogenic *CARD11* mutations in human diffuse large B cell lymphoma. *Science* **319**, 1676–1679 (2008).
- Deacon, E. M. *et al.* Epstein-Barr virus and Hodgkin's disease: transcriptional analysis of virus latency in the malignant cells. *J. Exp. Med.* **177**, 339–349 (1993).
- Yin, M. J. *et al.* HTLV-I Tax protein binds to MEK1 to stimulate I $\kappa$ B kinase activity and NF- $\kappa$ B activation. *Cell* **93**, 875–884 (1998).
- Isaacson, P. G. & Du, M. Q. MALT lymphoma: from morphology to molecules. *Nature Rev. Cancer* **4**, 644–653 (2004).
- Skininger, B. F. & Mak, T. W. The role of cytokines in classical Hodgkin lymphoma. *Blood* **99**, 4283–4297 (2002).

**Supplementary Information** is linked to the online version of the paper at [www.nature.com/nature](http://www.nature.com/nature).

**Acknowledgements** This work was supported by the Core Research for Evolutional Science and Technology, Japan Science and Technology Agency, by the 21<sup>st</sup> century centre of excellence program 'Study on diseases caused by environment/genome interactions', and by Grant-in-Aids from the Ministry of Education, Culture, Sports, Science and Technology of Japan and from the Ministry of Health, Labor and Welfare of Japan for the 3rd-term Comprehensive 10-year Strategy for Cancer Control. We also thank Y. Ogino, E. Matsui and M. Matsumura for their technical assistance.

**Author Contributions** M.Ka., K.N. and M.S. performed microarray experiments and subsequent data analyses. M.Ka., Y.C., K.Ta., J.T., J.N., M.I., A.T. and Y.K. performed mutation analysis of A20. M.Ka., S.Mu., M.S., Y.C. and Y.Ak. conducted functional assays of mutant A20. Y.S., K.Ta., Y.As., H.M., M.Ku., S.Mo., S.C., Y.K., K.To. and Y.I. prepared tumour specimens. I.K., K.O., A.N., H.N. and T.N. conducted *in vivo* tumorigenicity experiments in NOG/SCID mice. T.I., Y.H., T.Y., Y.K. and S.O. designed overall studies, and S.O. wrote the manuscript. All authors discussed the results and commented on the manuscript.

**Author Information** The copy number data as well as the raw microarray data will be accessible from the GEO (<http://ncbi.nlm.nih.gov/geo/>) with the accession number GSE12906. Reprints and permissions information is available at [www.nature.com/reprints](http://www.nature.com/reprints). Correspondence and requests for materials should be addressed to S.O. (sogawa-ky@umin.ac.jp) or Y.K. (ykkobaya@ncc.go.jp).